

Spatio-temporal variability of zooplankton standing stock in  
eastern Arabian Sea inferred from ADCP backscatter  
measurements

Ranjan Kumar Sahu, D. Shankar, P. Amol, S.G. Aparna, D.V. Desai

December 18, 2024

**Abstract**

The spatio-temporal variation of zooplankton biomass and standing stock in the eastern Arabian Sea (EAS) is mapped using backscatter measurements from 153.3 kHz acoustic Doppler current profiler (ADCP) moorings deployed at seven locations on the continental slope off the west coast of India from October 2017 to December 2023. The conversion from backscatter to biomass is based on volumetric zooplankton sampling at the respective locations. Analysis of the data over 24–120 m shows that the backscatter and zooplankton biomass decrease from the upper ocean ( $215 \text{ mg}^{-3}$  biomass contour) to the lower depths. Changes are observed in the seasonal variation of the monthly climatology of zooplankton standing stock (integral of the biomass over 24–120 m water column) as we move to poleward along the slope in EAS. The range of variation of standing stock is lowest at Kanyakumari, followed by Okha, which lie at the southern and northern boundary of the EAS,

<sup>12</sup> respectively. While annual cycle is predominant at northeastern Arabian Sea (NEAS), it decreases  
<sup>13</sup> towards southeastern Arabian Sea (SEAS) where the semi-annual cycle tends to dominate. Analysis  
<sup>14</sup> reveals weak presence of annual cycle in zooplankton biomass and it is dominated by intraseasonal  
<sup>15</sup> and intra-annual components. Intraseasonal variability is often comparable (stronger) to the intra-  
<sup>16</sup> annual (annual) variability both of which increases (decreases) poleward with an evident presence in  
<sup>17</sup> SEAS. Stronger intraseasonal variability has implication on zooplankton sampling, it's patchiness  
<sup>18</sup> and biomass predictability.

<sub>19</sub> **1 Introduction**

<sub>20</sub> **1.1 Background**

<sub>21</sub> Zooplankton plays a vital role in food web of pelagic ecosystem by enabling the hierarchical trans-  
<sub>22</sub> port of organic matter from primary producers to higher trophic levels impacting the fish population  
<sub>23</sub> [Ohman and Hirche, 2001] and the carbon pump of the deep ocean [Quéré et al., 2016]. They are  
<sub>24</sub> presumably the largest migrating organisms in terms of biomass [Hays, 2003] which occurs in diel  
<sub>25</sub> vertical migration (DVM). Zooplankton depend not only on phytoplankton but other environmen-  
<sub>26</sub> tal parameters (e.g. mixed layer depth, insolation, oxygen, thermocline, nutrient availability, chl-a  
<sub>27</sub> (chl-a) concentration and daily primary production). The biological productivity of the ocean is  
<sub>28</sub> essentially connected with physics and chemistry [Subrahmanyam, 1959, Ryther et al., 1966, Qasim,  
<sub>29</sub> 1977, Nair, 1970, Banse, 1995, McCreary et al., 2009, Vijith et al., 2016, Amol et al., 2020]. The  
<sub>30</sub> dynamic ocean results in varying physico-chemical properties, leading to bloom and growth of  
<sub>31</sub> plankton in favourable conditions. The changes are strongly influenced by the seasonal cycle in the  
<sub>32</sub> North Indian Ocean (NIO; north of 5 °N of Indian Ocean). The eastern boundary of Arabian Sea  
<sub>33</sub> contains the West India Coastal Current ([Ramamirtham and Murty, 1965, Banse, 1968, Shetye  
<sub>34</sub> et al., 1990, McCreary et al., 1993, Amol et al., 2014, Vijith et al., 2016, Chaudhuri et al., 2020,  
<sub>35</sub> WICC]) which reverses seasonally, flowing poleward (equatorward) during November to February  
<sub>36</sub> (June to September) ([Shetye et al., 1990, 1991, Vijith et al., 2022]).

<sub>37</sub> A direct consequence of this reversal is the seasonal cycle of thermocline ([Prasad and Bahu-  
<sub>38</sub> layan, 1996, Kumar and Narvekar, 2005]), oxycline ([DeSousa et al., 1996, Schmidt et al., 2020]) and  
<sub>39</sub> thickness of mixed Layer Depth (MLD) ([Shetye et al., 1991, Prasad and Bahulayan, 1996, Kumar  
<sub>40</sub> and Narvekar, 2005]) induced by upwelling (downwelling) favourable conditions in summer (winter)

41 at eastern Arabian Sea (EAS) facilitated further by wind speed and near-surface stratification. Fur-  
42 ther, the phytoplankton biomass and chl-a concentration changes with the season [Subrahmanyam  
43 and Sarma, 1960, Banse, 1968, Kumar and Narvekar, 2005, Lévy et al., 2007, Vijith et al., 2016].  
44 Upwelling in summer monsoon leads to maximum chl-a growth in the entire EAS [Banse, 1968,  
45 Banse and English, 2000, McCreary et al., 2009, Hood et al., 2017, Bemal et al., 2018, Shi and  
46 Wang, 2022]. During winter monsoon, the convective mixing induced winter mixed layer [Shetye  
47 et al., 1992, Madhupratap et al., 1996b, McCreary et al., 1996, Lévy et al., 2007, Shankar et al.,  
48 2016, Vijith et al., 2016, Keerthi et al., 2017, Shi and Wang, 2022] results in winter chl-a peak at  
49 NEAS while the downwelling Rossby waves modulate chl-a along SEAS albeit limited to coast and  
50 islands [Amol et al., 2020].

51 The zooplankton grazing peak is instantaneous with no time delay from peak phytoplankton  
52 production [Li et al., 2000, Barber et al., 2001], but its population growth lags [Rehim and Imran,  
53 2012, Almén and Tamelander, 2020] depending on its gestation period and other limiting aspects.  
54 While some studies suggest that the peak timing of zooplankton may not change in parallel with  
55 phytoplankton blooms [Winder and Schindler, 2004], others indicate that lag exists between primary  
56 production and the transfer of energy to higher trophic levels [Brock and McClain, 1992, Brock  
57 et al., 1991]. The conventional zooplankton measurements, where only few snapshot/s of the event  
58 is captured gives an incoherent or incomplete understanding in terms of spatio-temporal variation  
59 of zooplankton [Ramamurthy, 1965, Pionkovski et al., 1995, Madhupratap et al., 1992, 1996a,  
60 Wishner et al., 1998, Kidwai and Amjad, 2000, Barber et al., 2001, Khandagale et al., 2022] as  
61 much information is revealed by later studies [Jyothibabu et al., 2010, Shankar et al., 2019, Aparna  
62 et al., 2022] using high resolution data. Calibrated acoustic instruments such as acoustic Doppler  
63 current profiler (ADCP) along with relevant data can be utilised to understand small scale variability

64 [Nair et al., 1999, Edvardsen et al., 2003, Smith and Madhupratap, 2005, Smeti et al., 2015, Kang  
65 et al., 2024], the complex interplay between the physico-chemical parameters and ecosystem [Jiang  
66 et al., 2007, Potiris et al., 2018, Shankar et al., 2019, Aparna et al., 2022, Nie et al., 2023], the  
67 zooplankton migration [Inoue et al., 2016, Ursella et al., 2018, 2021] and their seasonal to annual  
68 variation [Jiang et al., 2007, Hobbs et al., 2021, Liu et al., 2022, Aparna et al., 2022].

69 The relationship between backscatter and the abundance and size of zooplankton was described  
70 by Greenlaw [1979] wherein it was pointed out that single frequency backscatter can be used to esti-  
71 mate abundance if mean zooplankton size is known. A drastic increase in study temporal and spatial  
72 variation of zooplankton biomass using backscatter-proxy came in 1990s by introduction of high-  
73 frequency echo sounders, with studies [Flagg and Smith, 1989, Wiebe et al., 1990, Batchelder et al.,  
74 1995, Greene et al., 1998, Rippeth and Simpson, 1998] methodically showing acoustic backscatter  
75 estimated zooplankton biomass. Net sampling augmented ADCP backscatter have been used to  
76 study DVM and the spatial and temporal variability of zooplankton biomass in different marine  
77 regions, such as the Southwestern Pacific, the Lazarev Sea in Antarctica and the Corsica Channel  
78 in the north-western Mediterranean Sea [Cisewski et al., 2010, Hamilton et al., 2013, Smeti et al.,  
79 2015, Guerra et al., 2019]. The first such study to exploit the potential of ADCPs in EAS was  
80 carried out by Aparna et al. [2022] (A22 from hereon) using ADCP moorings deployed on conti-  
81 nental slopes off the Indian west coast. In their work, they showed that the zooplankton standing  
82 stock (ZSS) in fact declines during upwelling facilitated increase in phytoplankton biomass. The  
83 unusual interaction implies the break down of existing understanding of predator-prey relationship  
84 in fundamental level of marine food chain.

85    **1.2 Objective and scope of the manuscript**

86    A network of ADCPs has been installed off the continental slope and shelf on the west coast of  
87    India. This ADCPs have enabled a rigorous view of intraseasonal to seasonal scale variability [[Amol](#)  
88    [et al., 2014](#), [Chaudhuri et al., 2020](#)] of WICC. In the recent study A22 have used ADCP moorings  
89    off Mumbai, Goa and Kollam to explain the temporal variability of zooplankton biomass. The  
90    study showed that the zooplankton peaks (and troughs) is not only non-uniform in latitude but  
91    also heavily influenced by the oxygen minimum zone, MLD and the seasonal upwelling/downwelling  
92    conditions. Stark contrast in the phytoplankton bloom and subsequence growth of zooplankton or  
93    the lack thereof was observed in the EAS regimes.

94    We extend the work of A22 by presenting data from four additional moorings in the EAS, show-  
95    casing the deviations of seasonal cycle from climatology, and discussing the significant intraseasonal  
96    variability of biomass and standing stock revealed by the ADCP data. The paper is organized as  
97    follows; datasets and methods employed are described in section 2. Section 3 describes the observed  
98    climatology of zooplankton biomass and standing stock. A comparison is drawn to the results of  
99    A22. Further, the seasonal cycle of zooplankton biomass and standing stock is discussed with re-  
100   lation to the MLD, oxygen, temperature and circulation in determining the biomass is discussed  
101   in results section 4. Section 5 delves deeper into the intraseasonal variability with summary and  
102   conclusion in section 6.

103   **2 Data and methods**

104   The backscatter data from ADCP and the zooplankton samples collected from the periphery of  
105   mooring is described in this section. The backscatter derived from the echo intensity of the seven

106 ADCP mooring deployed on the continental slope off the Indian west coast is the primary data we  
107 have use in this manuscript. The moorings details are summarized in [Table 1](#). In situ biomass data  
108 from volumetric zooplankton samples are used to validate and correlate with backscatter. The chl-a  
109 data is used to study and draw inferences for the possible zooplankton growth seasons. In addition,  
110 we have used the monthly climatology of temperature and salinity from [Chatterjee et al. \[2012\]](#).

## 111 2.1 ADCP data and backscatter estimation

112 The ADCPs were deployed on the continental slope off the Indian west coast ([Fig. 1](#)), off Mumbai,  
113 Goa, Kollam and Kanyakumari, and later extended to three more sites to cover the entire EAS  
114 basin from Okha ( $22.26^{\circ}\text{N}$ ) in north to Kanyakumari ( $6.96^{\circ}\text{N}$ ) in south. The other two ADCPs  
115 are, 1) Jaigarh at central EAS (CEAS), 2) Udupi (primarily at SEAS regime) in the transition  
116 zone between CEAS and SEAS. The extended moorings were deployed in October 2017, though  
117 Kanyakumari had been deployed earlier too. However, only Mumbai, Goa and Kollam were part of  
118 the previous backscatter study by A22. The moorings are serviced on yearly basis usually during  
119 October–November or sometime during September–December (depending on ship availability). The  
120 ADCPs are of Teledyne RD Instruments make, upward-looking and operate at 153.3 kHz. While  
121 utmost care is taken to position the instrument (mooring) at  $\sim$ 150–200 m ( $\sim$ 1050–1100 m) depth,  
122 yet for some deployments it's shallow or deeper owing to drift caused by floater buoyancy-anchor  
123 weight balance. Data was collected at hourly interval and the bin size was set to 4 m. The echoes at  
124 surface to 10% range ( $\sim$ 20 m) means the data at these depths is rendered useless and is discarded  
125 from further use. We have followed the methodology laid down in A22 to derive the backscatter  
126 time series from ADCP echo intensity data. The gaps up to two days are filled using the grafting  
127 method of [Mukhopadhyay et al. \[2017\]](#) once the zooplankton biomass time series is constructed.

128 **2.2 Zooplankton data and estimation of biomass**

129 The zooplankton samples were collected in the vicinity ( $\sim 10$  km) of ADCP mooring site twice,  
130 once prior retrieval and again post deployment of moorings so that there is overlap in the ADCP  
131 time instance and in situ zooplankton samples during servicing cruises on board of RV Sindhu  
132 Sankalp and RV Sindhu Sadhana ([Table 2](#)). Multi-plankton net (MPN) (100  $\mu\text{m}$  mesh size, 0.5  $\text{m}^2$   
133 mouth area) was used to get samples in the pre-determined depth ranges; water volume filtered was  
134 calculated by the product of sampling depth range and the mouth area of net. The depth range  
135 and timing of sample collection was different throughout the MPN hauls (refer [Table 2](#)). From  
136 2020 onward, the depth-range was standardized to the bins of 0–25, 25–50, 50–75, 75–100, 100–150  
137 (units are in meters). The backscatter obtained earlier is averaged in vertical corresponding to the  
138 specific MPN hauls for each site. The backscatter is linearly regressed with respective biomass to  
139 establish their relationship ([Fig. 2](#)), which has been demonstrated in numerous previous studies  
140 [[Flagg and Smith, 1989](#), [Heywood et al., 1991](#), [Jiang et al., 2007](#), [Aparna et al., 2022](#)].

141 **2.2.1 Biomass time series and estimation of standing stock**

142 The zooplankton biomass time series ([Fig. 3](#)) is created from the above derived linear relationship.  
143 The standing stock is determined by taking the depth integral of biomass over the water column.  
144 To maintain the consistency of standing stock estimation, only those deployments that doesn't lack  
145 data at any depth in the entire range of 24–120 m are considered for analysis as in A22. The lack of  
146 data in the above mentioned depth range is due to deviation in positioning of ADCP sensor in the  
147 water column. A swift alteration in bathymetry along the continental slope implies that the mooring  
148 might anchor at a different depth than planned, hence a change in the predicted position of ADCP.  
149 This leads to gap in data at few mooring sites for some year. For example, for the northern-most

150 mooring at Okha, data is not available for the entire upper 120 m depth for the second deployment.  
151 Also at Jaigarh, where the surface to ~60 m data (in 3rd deployment) and Kollam, where 80 m  
152 and below (in 4th deployment) is unavailable and hence discarded from standing stock estimation.  
153 There are few deployments where no or bad data was recorded e.g, at Udupi (4th deployment) and  
154 Kanyakumari (6th deployment).

### 155 **2.3 Mixed-layer depth, temperature, oxygen and chlorophyll**

156 As we are using a 153.3 kHz ADCP moored at ~150 m, the top ~10% of data is unusable because  
157 of surface echoes. MLD in EAS is of the order ~20 to 40 m during summer monsoon [Shetye et al.,  
158 1990, Shankar et al., 2005, Sreenivas et al., 2008] especially in the SEAS [Shenoi et al., 2005], but  
159 during winter the MLD in northern NEAS remains deep [Shankar et al., 2016]. The temperature  
160 data is used from Chatterjee et al. [2012], a monthly climatology having 1° spatial resolution.  
161 Monthly climatology of oxygen data is obtained from World Ocean Atlas 2013 [García et al., 2014]  
162 which contains objectively analyzed 1° climatological fields of in situ measurements. Previous  
163 study based on ADCP data of EAS A22 have used SeaWiFS based chl-a data for comparison with  
164 climatology of ZSS. The SeaWiFS was at its end of service in 2010, hence we use new chl-a product  
165 from Global Ocean Colour, biogeochemical L3 data obtained from [E.U. Copernicus Marine Service](#)  
166 [Information](#). The daily data is available at a spatial resolution of 4 km.

## 167 **3 Time series, climatology and seasonal cycle**

168 A decrease in biomass with increasing depth at all seven study sites is observed ([Fig. 3](#)). To  
169 distinguish between high and low productivity zones, we employed a biomass contour, similar  
170 to the 215 mg m<sup>-3</sup> threshold used in A22. However, to better capture seasonal variations off

<sup>171</sup> Kanyakumari and Okha, the threshold was replaced by  $175 \text{ mg m}^{-3}$ . The biomass contour z215  
<sup>172</sup> (depth contour D215) and z175 (depth contour D175) allows us to link the seasonal variation  
<sup>173</sup> of biomass to the physico-chemical properties. The monthly climatology of biomass and ZSS is  
<sup>174</sup> computed for all locations having valid data in 24–140 m depth range. Climatology of zooplankton  
<sup>175</sup> biomass and ZSS is discussed at locations northward starting from southernmost mooring site i.e,  
<sup>176</sup> Kanyakumari. Time series, climatology and seasonal cycle of biomass is discussed in the following  
<sup>177</sup> subsection 3.2. For a comparison with physico-chemical forcing similar to A22, we use isotherm of  
<sup>178</sup>  $23^\circ\text{C}$  (henceforth, D23) and oxygen contour specific to each site depending on its position relative  
<sup>179</sup> to oxygen minimum zone (OMZ) boundaries of EAS.

### <sup>180</sup> 3.1 Time series description

<sup>181</sup> Rate of biomass decrease with depth, roughly defined as the difference between mean biomass at 40  
<sup>182</sup> and 104 m depth is highest off Jaigarh and Mumbai as it has higher biomass in upper ocean ([Fig. 4](#))  
<sup>183</sup> and lowest off Kanyakumari. This is followed by Goa and Udupi. While the biomass decrease with  
<sup>184</sup> depth is lower off Kollam from 2017 to 2020, it becomes considerably high from thereon ([Fig. 4 f](#)).  
<sup>185</sup> A comparatively moderate decline in zooplankton biomass with respect to depth off Okha ([Fig. 3](#)  
<sup>186</sup> a1, a2) at NEAS is agreeing with earlier reported data [[Wishner et al., 1998](#), [Madhupratap et al.,  
<sup>187</sup> 2001](#), [Smith and Madhupratap, 2005](#), [Jyothibabu et al., 2010](#)]. The difference of mean biomass at 40  
<sup>188</sup> and 104 m is high at most location but it arises due to the bigger difference in select few years, e.g.,  
<sup>189</sup> off Mumbai during 2020 and 2022, off Jaigarh in 2021, at Goa during 2021–2022, off Kollam during  
<sup>190</sup> 2022. The sites at SEAS, particularly off Kanyakumari for all years and 2017 to 2020 off Kollam  
<sup>191</sup> also have weaker decrease [[Madhupratap et al., 2001](#), [Jyothibabu et al., 2010](#), [Aparna et al., 2022](#)].  
<sup>192</sup> However, the biomass decline with depth post 2021 off Kollam is high owing to a strong bloom in

these years and is reflected as D215 deepening. D175 and D215 is deep throughout EAS during winter monsoon as seen from the same biomass value at 40 and 104 m indicating the penetration of D215/D175 all the way to 104 m, but the occurrence of high biomass is distinct to each regime of EAS. Upper ocean shows considerably high biomass and ZSS during winter monsoon at NEAS. On the contrary at SEAS, the upper ocean shows higher biomass during summer monsoon even though the D215 and D175 is shallower during this period.

The mean, standard deviation of biomass, ZSS and chl-a are shown in supplementary table S1. There is no consistent variation as seen from the analysis of mean and standard deviation of biomass at 40 and 104 m. The sites with higher biomass tends to have higher variation over time e.g. Mumbai, Jaigarh and Kollam. Superposed on the time-series is seasonal cycle and variability of distinct period band, a discussion is presented in [subsection 3.3](#). Variation in the monthly average or seasonal cycle over time suggests presence interannual variability.

### 3.2 Climatology of zooplankton biomass and standing stock

Off Kanyakumari, z175 is shallower from May onward till October and the zooplankton biomass is comparatively higher than rest of the year ([Fig. 5 g1](#)). The D23 isotherm along-with oxycline (marked by  $2.1 \text{ ml L}^{-1}$ , a higher oxygen contour as it lies outside OMZ core) follows the same seasonal cycle like D175. However, there is almost no seasonal variation in ZSS off Kanyakumari ( $\sigma, 0.67 \text{ gm m}^{-2}$ ) as compared to the chl-a variation ( $\sigma, 1.53 \text{ mg m}^{-3}$ ). At the nearest northern mooring site off Kollam, a strong seasonal cycle is observed and the D215 is deeper for any given month. A decline (steep-rise) in ZSS (chl-a biomass) is seen and its minimum (peak) is attained in August ([Fig. 5 f2](#)). This feature was previously reported by A22, highlighting an imbalance in the interaction between zooplankton and phytoplankton, it occurs due to shallowing of thermocline

215 and low oxygen, and that's why the ZSS is at it's minimum when chl-a peaks. A similar feature is  
216 seen further north, off Udupi which sits at the transition zone of SEAS and CEAS, albeit with a  
217 relatively weaker zooplankton biomass and minimum (peak) of ZSS (chl-a) occurring a month later  
218 during September.

219 The D215 seasonal trend off Goa in present study is similar to trend of D215 off Goa as described  
220 in A22 (See section S1 of supplementary for comparison). The biomass off Goa decreases rapidly  
221 below the z215 as reported earlier, reaching as low as  $60 \text{ mg m}^{-3}$  at 130 m during June to September  
222 ([Fig. 5 d1](#)). The ZSS off Jaigarh is identical but stronger to that of off Goa, owing to higher biomass  
223 above z215 and the comparatively deeper D215 ([Fig. 5 c1](#)). What's intriguing is a presence of strong  
224 variation in ZSS off Jaigarh ( $\sigma, 3.24 \text{ gm m}^{-2}$ ) highest among all locations although the seasonal  
225 variation in chl-a biomass ([Fig. 5 c2](#)) is visibly non-existent ( $\sigma, 0.05 \text{ mg m}^{-3}$ ) and lowest among  
226 all locations. This is an exact opposite scenario of Kanyakumari, where an insignificant seasonal  
227 variation in ZSS is seen even though the chl-a biomass varies strongly. Starting from Kollam ([Fig. 5](#)  
228 f1) and moving northward to Jaigarh ([Fig. 5 c1](#)), we see that the core of high zooplankton biomass  
229 gradually shifts from summer (off Kollam) to winter monsoon (off Jaigarh), with the transition of  
230 upper ocean zooplankton biomass happening along Udupi and Goa. On the contrary, chl-a biomass  
231 tends to have low seasonal range as we move northward from SEAS, with Jaigarh having the least  
232 seasonal variation. This shift along with winter monsoon facilitated deeper thermocline leads to an  
233 even larger impact on ZSS.

234 Further north off Mumbai the D215 is deeper in December to early April, resulting in a  
235 higher ZSS ([Fig. 5 b2](#)). D23 follows D215 and the oxycline follows an erratic pattern, reaching  
236 depths  $> 140 \text{ m}$  during January to March; when a higher biomass is observed above z215. The  
237 chl-a biomass shows seasonal variation albeit lower than the SEAS counterpart. At the northern-

238 most site of EAS i.e, off Okha, biomass above z175 is much weaker leading to a relatively lower  
239 ZSS ([Fig. 5](#) a1, a2) compared to Mumbai. There's two chl-a peak off Okha, one in February due to  
240 convective mixing induced deepening of MLD [[Wiggert et al., 2005](#), [Lévy et al., 2007](#), [Keerthi et al.,](#)  
241 [2017](#), [Shankar et al., 2016](#)] and the other during August in summer monsoon [[Wiggert et al., 2005](#),  
242 [Lévy et al., 2007](#)]. The ZSS remains flat during June to September, although the chl-a biomass  
243 increases in this time. Afterwards, ZSS gradually increases and attains its maximum in February  
244 same as the chl-a biomass. For a discussion on comparison with A22 climatology, the readers are  
245 referred to supplementary section S1.

### 246 3.3 Seasonal cycle and variability

247 The deviations from climatology represent the seasonal cycle. This section will deal with a discussion  
248 on the seasonal cycle and variability of biomass and ZSS in annual and intra-annual scale along  
249 the three regimes of EAS. To understand the variation at a specific period, say 365-days (annual  
250 cycle) or 180-days (semi-annual cycle), wavelet analysis is carried out for biomass ([Fig. 6](#)) and ZSS  
251 ([Fig. 7](#)). However, if we wish to understand the variation in a specific period band, we use Lanczos  
252 filtered time series. A brief discussion on the above mentioned techniques and variability in distinct  
253 period band is given in supplementary Section S2.

254 From the linear equation correlating biomass and backscatter, the upper and lower bound of  
255 error limits equals to  $\sim 14 \text{ mg m}^{-3}$  ([Fig. 2](#)). The standard deviation of intra-annual (annual)  
256 variability is comparable to (less than) the error range of biomass vs backscatter relation. However,  
257 we are limited by the gaps in time series as discussed in [subsubsection 2.2.1](#). Therefore, we consider  
258 locations other than Okha and Jaigarh for the 40 m biomass and ZSS in annual scale.

259 The seasonal cycle is the sum total of annual, semi-annual cycle and their variability. The

annual cycle of biomass off Kanyakumari (Udupi and Kollam) is weak (strong), but it varies in time ([Fig. 6](#)). For example off Kollam, the wavelet power is stronger post 2020. Wavelet analysis of the ZSS time series, derived from integrated biomass between 24 and 120 meters depth, indicates absence (presence) of annual cycle off Kanyakumari (off Udupi) ([Fig. 7 g1](#)). To capture the annual variability, the biomass is passed through Lanczos filter within period of 300 to 400 days ([Fig. 8](#)). The annual variability off Kanyakumari is least among all mooring sites. Kollam shows strong annual variability indicating prominent year-to-year variation of biomass. The intra-annual band ([Fig. 9](#)) tends to be stronger compared to the annual band. Much like the annual cycle, the semi-annual cycle is weak and intra-annual variability is moderate off Kanyakumari compared to Kollam and Udupi. However, the strong variability in intra-annual scale is restricted to upper ocean for few years off Kollam, where minor spectra around 120 days is also observed.

Off Goa, the annual cycle of biomass is comparatively weak contrary to the results of A22, possibly due to shorter time record and low biomass in the recent years as reflected in its ZSS wavelet for 2018 to early 2020 (2021 and 2022) ([Fig. 7](#)) resulting in a weak (strong) annual variability ([Fig. 8](#)). Off Goa and Jaigarh, the semi-annual cycle tends to be strong, specifically during 2022 when a anomalous bloom is observed throughout EAS. The semi-annual cycle weakens with depth in these locations. Intra-annual component of seasonal cycle is observed off Goa, with weak (strong) variability during 2019 (2020, 2022) and is moderately strong off Jaigarh ([Fig. 9](#)). Energy is spread among all intra-annual periods for 2022 off Goa ([Figs. 6 and 7](#)), while during 2019 and 2020 the wavelet energy is only present in the semi-annual periods resulting in a overall weaker intra-annual component ([Fig. 6](#)).

Further north, a strong annual cycle is seen off Mumbai with strong annual variability highest among EAS sites ([Fig. 8](#)). Biomass variability in annual scale decreases minutely with depth off

283 Mumbai and the three CEAS sites than off Kollam ([Fig. 8](#)) similar to the observed ocean currents  
284 [[Chaudhuri et al., 2020, 2021](#)]. The annual cycle and annual variability of biomass and subsequently,  
285 ZSS increases along the slope as we go northward to Mumbai from Kanyakumari. The intra-annual  
286 band's strength is reduced off Mumbai and Okha as compared to CEAS and SEAS, and the intra-  
287 annual variability also decreases more with depth as we go equatorward. The semi-annual cycle is  
288 moderately present at 40 m off Mumbai which weakens at 104 m resulting in higher contribution of  
289 annual cycle to ZSS. Analysis reveals the presence of moderately strong semi-annual cycle off Okha  
290 but only at 104 m and it's intra-annual (annual) band is similar (weaker) in magnitude as compared  
291 to Mumbai. Excluding Kanyakumari, intra-annual variability of biomass decreases poleward with  
292 higher variation seen off Kollam and Udupi similar to the WICC [[Amol et al., 2014, Chaudhuri](#)  
293 [et al., 2020](#)].

## 294 4 Intraseasonal variability

295 On the similar lines as discussed in the preceding section, intraseasonal variability of biomass is  
296 defined as shifts occurring within a season, typically lasting few days to few weeks and is driven  
297 by short-term environmental changes, e.g., nutrient replenishment (depletion) in short-span due to  
298 upwelling and/or entrainment (bloom). The variability can be split into two categories; a high-  
299 frequency (period < 30 days) and a low-frequency (30 < period < 90 days) component. The  
300 presence of significant variation in the 30-day running mean with recurring bursts are seen in the  
301 daily data and in the wavelet analysis of biomass at 40 and 104 m ([Fig. 6](#)) lasting few days to  
302 a week and distinctive to each location. Most of the spikes in biomass are occurring due to the  
303 high-frequency component of intraseasonal band, but our focus is on the low-frequency component  
304 seen as bursts lasting much longer than biomass spikes. Much like the intra-annual variability,

305 the standard deviation of intraseasonal component is comparable or higher than the error range of  
306 unfiltered biomass vs backscatter relation.

307 The strength and contribution of variability components changes over time and differs between  
308 EAS regimes as discussed in [subsection 3.3](#). From the wavelet analysis of biomass at 40 and  
309 104 m, peaks in low-frequency intraseasonal band is observed across EAS. But the variability can  
310 be different at upper and lower regimes at a given location within a specific period band. This  
311 difference is evident e.g., during 2019–2021 off Kanyakumari, the wavelet power of biomass within  
312 the intraseasonal band declines as we go deeper from 40 m ([Fig. 6](#)). The filtered biomass in  
313 intraseasonal band also showcases the decrease in variability with respect to depth for the same  
314 period off Kanyakumari ([Fig. 10](#)). This holds true across EAS with the exception of very few  
315 years where the variability at 104 m is comparable or higher than biomass variability at surface  
316 layers. However, in other few instances, such as during September–November of 2018 off CEAS,  
317 intraseasonal variability remains consistent throughout the entire water column.

318 Strong intraseasonal variability off Kanyakumari relative to the variability in its annual band,  
319 along-with comparable or lower range of intra-annual variability ([Fig. 11](#)) and the wavelet at 40  
320 and 104 m indicates that the short-lived environmental changes is a major driver of its biomass  
321 alongside minor seasonal variation. Off Kollam and Udupi, the presence of intraseasonal bursts is  
322 prominent, but due to an equal strength of intra-annual component the biomass isn't solely driven  
323 by short-term environmental changes. For instance, in 2019 off Kollam ([Fig. 11](#)), low frequency  
324 intraseasonal variability was weak during summer monsoon but an increase in biomass during the  
325 same period was due to an increase intra-annual component. However, a sharp decline in August  
326 2019 resulted from reduced intra-annual and intraseasonal variability, even with the presence of a  
327 weakly positive annual variability.

328 Off Goa, strong peaks in intraseasonal band is present in wavelet spectra of biomass. However,  
329 during early 2019 to late 2020, the intra-annual variability off Goa is non-existent and with the weak  
330 annual variability ([Fig. 11](#)), a rather invariant biomass at 40 m is observed ([Fig. 4](#)). The wavelet  
331 peaks in intraseasonal band occurred strongly in 2018 and later in 2020, but the absence intra-  
332 annual band in 2019 makes it easier to comprehend the contribution of intraseasonal variability. A  
333 similar feature is noted off Jaigarh albeit with a weaker magnitude.

334 Weak presence of intraseasonal variability is noticed in the relatively smoother 30-day rolling  
335 mean biomass off Mumbai and Okha. During early 2021 off Mumbai, the presence of strong intrasea-  
336 sonal peaks in wavelet spectra of 104 m along with 40 m ([Fig. 6](#)) shows up in biomass variability  
337 in intraseasonal scale ([Fig. 10](#)). Although spectra in the intraseasonal band is present at 40 m off  
338 Mumbai and Okha, it is almost absent at 104 m except for a select few years. It implies that at some  
339 locations the strong variability may occur at deeper depth even when the upper ocean is showing  
340 lower variability. Off Okha, the intraseasonal variability is lowest among all EAS sites followed by  
341 Mumbai. However, Okha has weak annual and intra-annual variability unlike Mumbai leading to  
342 least predictability.

343 The biomass variability at 40 and 104 m in intraseasonal scale is also reflected in the ZSS time  
344 series and the corresponding wavelet spectra ([Fig. 7](#)). No annual and semi-annual cycle seems  
345 to be present in ZSS off Kanyakumari, but presence of bursts lasting few days to weeks are an  
346 indication of intraseasonal variations. While off Kollam and Udupi, the presence of strong intra-  
347 annual variations is observed in ZSS alongside intraseasonal variation dominating specifically during  
348 September–November. Similarly, off Goa during early 2019 to late 2020 when the intra-annual and  
349 annual variations are much weak, strong intraseasonal variation leads to bursts in biomass. However,  
350 the strength of intraseasonal variability is reduced at NEAS leading to a comparatively smoother

351 ZSS in 30 day rolling mean window.

352 The intraseasonal peaks in biomass and further ZSS are strong in SEAS followed by CEAS and  
353 is weak off NEAS sites ([Fig. 10](#)). Variability in intraseasonal scale seems to occur predominantly  
354 during August to November, for example off Kanyakumari (2018, 2019 and 2020), off Kollam (2018,  
355 2021 and 2022) and off Udupi (2018) although it can extend to mid-summer/mid-winter monsoon  
356 for few years and is coherent along much of the EAS slope as seen during 2018 at intraseasonal band  
357 or sometimes even at scale of few days ([Fig. 11](#)). The coherence and strong variability at deeper  
358 depths at instance (during early 2021 off Mumbai) indicates possible role of ocean circulation in  
359 determining biomass at intraseasonal periods. Also, the magnitude of intraseasonal variability of 40  
360 m (104 m) biomass decreases (increases) as we move poleward ([Fig. 11](#)), the 40 m variance is much  
361 like the observed intraseasonal currents [[Amol et al., 2014](#), [Chaudhuri et al., 2020, 2021](#)]. However,  
362 the strength of intraseasonal variability of biomass is in contrast to the corresponding band of  
363 WICC which is strong during winter monsoon along the slope [[Amol et al., 2014](#), [Chaudhuri et al.,  
364 2020](#)] and shelf [[Chaudhuri et al., 2021](#)] suggesting further study to identify any possible connection.  
365 Nonetheless, the backscatter derived biomass in higher sampling frequency is essential for discussing  
366 the intraseasonal variability, whereas conventional sampling method such as with research vessel,  
367 where one snapshot of biomass is taken in an interval of 15–30 days, would fail to capture these  
368 bursts in biomass.

369 **5 Discussion**

370 **5.1 Summary**

371 The zooplankton biomass and standing stock across different regions of EAS was examined in this  
372 article, highlighting their spatio-temporal trends in the light of physico-chemical parameters using  
373 the multi-yearlong ADCP backscatter data from 2017 to 2023.

374 The findings shows notable seasonal variation in zooplankton biomass and ZSS; in SEAS the  
375 higher biomass is observed during summer monsoon, while in NEAS the high biomass is observed  
376 during winter monsoon with transition of peak biomass happening gradually along CEAS ([subsection 3.2](#)). Off Kollam, a unique double peak in ZSS occurs, one during May to July and another in  
377 September to November, suggesting a complex interplay between environmental drivers and zoo-  
378 plankton growth ([Fig. 5 f2](#)). Off Kanyakumari, the seasonal variation in ZSS is non-existent even  
379 though a dramatic seasonality is seen in chl-a. On contrary, Jaigarh shows strong variation in ZSS  
380 where the chl-a variation is non-existent. Such feature was observed at embayment west off Antarc-  
381 tic peninsula and has been attributed to advective influx [[Espinasse et al., 2012](#)] but the distinct  
382 dynamics of EAS and Antarctica implies the causality may not be same. Climatology shows strong  
383 decline in biomass w.r.t. depth off Goa, then NEAS sites off Jaigarh, Mumbai and Okha followed  
384 by SEAS locations off Udupi, Kollam and Kanyakumari. The minor peak observed off Mumbai in  
385 A22's climatology is absent in the climatology presented using the recent data.

387 Seasonal cycle and variability play a crucial role in regulating biomass. A strong annual cycle  
388 is observed at NEAS ([Fig. 6](#)), with biomass peaking during winter monsoon months ([Fig. 5](#)) and  
389 deeper D215, the annual cycle weakens as we got equatorward. CEAS and SEAS regions particularly  
390 off Kollam, exhibit more complex patterns. Off Kollam, the presence of a weak annual cycle and

391 a stronger semi-annual cycle is noted along with a moderately strong biennial cycle. The semi-  
392 annual cycle is especially prominent in the SEAS ([subsection 3.3](#)), where it contributes significantly  
393 to the seasonal biomass changes. The variability in annual scale is weak, while that in intra-  
394 annual scale is often comparable to intraseasonal variability which is found to influence zooplankton  
395 biomass strongly in the summer to winter monsoon transition months ([Fig. 10](#)). The high (low)  
396 frequency component of intraseasonal variability determine changes lasting for days (few days to  
397 weeks) observed as spikes (bursts) in the daily biomass record ([Fig. 11](#)). Intraseasonal variability is  
398 higher in the SEAS, with the NEAS displaying less variance. The intraseasonal variability is often  
399 restricted to the upper layer, and it is expected owing to higher variability of chl-a at surface which  
400 weakens with increasing depth. The affect of intraseasonal variability compounded with presence  
401 of strong intra-annual is observed in the difference of mean biomass at 40 and 104 m ([Fig. 4](#)). The  
402 intraseasonal variations may exist throughout the water column for few years and can be coherent  
403 along the slope possibly suggesting that the penetration and propagation of currents in intraseasonal  
404 band ([[Amol et al., 2012, 2014, Chaudhuri et al., 2020](#)]) could be driving biomass on few occasions.

## 405 **5.2 consequences of intraseasonal variability**

406 It is evident that the intraseasonal variability dominates the zooplankton biomass along EAS regime  
407 ([section 4](#)). A strong intraseasonal component suggests implications on sampling, zooplankton  
408 patchiness and its predictability.

### 409 **5.2.1 Implication on sampling**

410 Zooplankton biomass exhibits significant intraseasonal variability driven by dynamic oceanographic  
411 processes which operate over short temporal scales and vary in space ([section 4](#)). Since the strength

412 of intraseasonal component is higher than the other two variabilities ([Fig. 11](#)) and its high-frequency  
413 component is rather erratic, dependency of zooplankton biomass on the intra-seasonal variation  
414 has implication on the sampling of zooplankton using cruises. A servicing cruise along the EAS  
415 moorings takes about 12 to 15 days excluding the time to and fro from port to first/last mooring  
416 [[Chaudhuri et al., 2020](#), [Aparna et al., 2022](#)]. However, a sampling cruise dedicated to study the  
417 spatial variation of zooplankton [[Madhupratap et al., 1992](#), [Smith et al., 1998](#), [Wishner et al., 1998](#),  
418 [Kidwai and Amjad, 2000](#)], say for summer monsoon may last a month or more with coarse sampling  
419 interval and hence fail to capture the actual biomass within a season for a fair spatial comparison.

420 Consider the cruise undertaken to address the seasonality in zooplankton abundances and com-  
421 position [[Madhupratap et al., 1996a](#)] in Arabian Sea as part of JGOFS program. The first, second  
422 and third cruises of this study was taken 12 April to 12 May 1994 (inter-monsoon), 3 February to  
423 4 March 1995 (winter) and 20 July to 12 August 1995 (summer), respectively. It is imperative to  
424 acknowledge that sampling done twice (once in mid-day and again in mid-night), and two snapshots  
425 are held as a representative of the entire season. Does this sampling method give accurate idea  
426 about the zooplankton biomass in a particular season? The comparison of variability in intrasea-  
427 sonal periods is used to shed a light on the biomass variation within a season. Consider the summer  
428 monsoon months, off Mumbai during early June of 2019 ([Fig. 11](#)), where a spike in biomass is  
429 observed due to an instantaneous increase in the high-frequency component of biomass variability  
430 resulting in an increase of  $\sim 150 \text{ mg m}^{-3}$  within few days. Similar spikes are seen at other locations  
431 too, e.g., off Kollam during July end and multiple instances in September of 2019 ([Fig. 11](#)). These  
432 spikes lasts only for a day to few days but the bursts in biomass tend to last longer from a few  
433 days to a few weeks. A burst is seen in biomass during September 2019 off Kanyakumari, but  
434 the preceding summer monsoon months had an almost invariant biomass with minor bursts, both

435 of which won't be captured by a conventional ship based sampling. Second limitation of cruise  
436 based sampling is spatial constraint. For the same year 2019 off Kanyakumari, the burst in biomass  
437 during September is followed by a decline during October which results in a biomass difference of  
438 about  $\sim 160 \text{ mg m}^{-3}$  within a month and most of it is contribution from intraseasonal variability  
439 ([Fig. 11](#)). This burst is also observed off Kollam, Udupi till Goa, albeit with decreasing intensity  
440 as we go poleward. Such coherency can only be observed if continuous and frequent measurements  
441 were taken across EAS. The spatial map of mesozooplankton distribution such as one by [Jyothi-](#)  
442 [babu et al. \[2010\]](#) for each season (see Fig. 11 of [Jyothibabu et al. \[2010\]](#)) is limited by sampling  
443 frequency and time elapsed to cover stations, and the measured biomass is prone to distortion since  
444 biomass is subject to drastic changes within few days. The limitations of cruise based sampling  
445 leads to inaccurate depiction of biomass in space and time, and it can be mitigated by usage of  
446 ADCP backscatter derived zooplankton biomass.

#### 447 **5.2.2 Zooplankton patchiness**

448 Poor sampling coverage and intermittent measurement also impacts assessment of zooplankton  
449 patchiness, defined as the aggregations arising in response to temperature, salinity and oxygen gra-  
450 dients, currents, variation in light intensity, predator-prey concentrations [[Folt and Burns, 1999](#),  
451 [Raghukumar and Anil, 2003](#)]. Though the usage of traditional sampling methods has led to de-  
452 termination of zooplankton abundance and distribution in EAS [[Madhupratap et al., 1992, 1996a](#),  
453 [Khandagale et al., 2022](#)], the biomass measurements can miss or rarely sample the patches of zoo-  
454 plankton, and thereby misinterpret abundance by under/over-estimation of the standing stock. A  
455 high intraseasonal variability in zooplankton biomass suggests that patchiness in the deep-sea en-  
456 vironment occurs within individual seasons on periods equivalent to few days to few weeks. During

457 July 20–31st 2019, a spike lasting few days in daily biomass at 40 m ([Fig. 11](#)) is observed at most  
458 of the EAS sites, albeit with differing magnitude followed by a sharp decline and difference in oc-  
459 currence of maximum biomass by few days. But the coherence doesn't exist at all instances. For  
460 example, during 13th June 2019, the instantaneous spike in biomass observed off Mumbai is not  
461 seen anywhere else, but the low biomass lasting about 2 weeks in dates adjacent to this spike is  
462 seen at Okha, Mumbai, Jaigarh and Goa ([Fig. 11](#)). The observed spikes in zooplankton biomass,  
463 as discussed in the preceding subsection, occurring within just a few days, are a clear example  
464 of the zooplankton cluster formation. The patchiness can also exist on longer periods. During  
465 15 January–15 February 2019, a burst is observed off Udupi lasting about 20–30 days, while it is  
466 missing at its nearby moorings, signifying presence of patchiness and its prominence in the longer  
467 periods of intraseasonal band. However, there are occasions such as during September–November  
468 2018 ([Fig. 10](#)) and 2019 ([Fig. 11](#)) when the coherence in biomass is observed indicating collapse of  
469 patchiness.

470 The zooplankton patchiness occurring in longer periods of intraseasonal band is likely associated  
471 with processes such as fronts [[Coyle and Jr, 2000](#), [Wade and Heywood, 2001](#), [Hitchcock et al., 2002](#)],  
472 pulsed inputs of nutrients in open ocean water [[Anil et al., 2021](#)] and biological processes [[Folt and](#)  
473 [Burns, 1999](#)], while those occurring in shorter periods could be due to physical convergence [[Napp](#)  
474 [et al., 1996](#)] of zooplankton. The higher variance in deeper layers off Okha could be an indication  
475 of deep-living zooplankton species [[Raghukumar and Anil, 2003](#)] due to strong oxygen gradient.  
476 Thus, a lack of feasibility in intensive in-situ sampling suggests that the data collected might not be  
477 representative of the actual standing stock being studied [[Smith et al., 1998](#)] and may not capture  
478 zooplankton patches.

479    **5.2.3 Predictability**

480    Though EAS shows a strong seasonal cycle of current, there are notable differences between regimes  
481    of EAS. Kollam's seasonal cycle is marked by intense intraseasonal bursts making the shelf WICC  
482    at Kollam highly unpredictable [Chaudhuri et al., 2021] and the intraseasonal variability increases  
483    equatorward. The direction of WICC at any given time of the year can be either poleward or  
484    equatorward owing to the bursts. Similarly, the zooplankton biomass varies frequently and strongly  
485    within the season itself ([section 4](#)) across EAS. From the preceding subsection, it is inferred that  
486    though not often, coherence is observed in both the lower and higher periods of intraseasonal band  
487    leading to collapse of patchiness. The presence of coherence implicates better predictability of  
488    biomass especially during September–November as observed during 2018 and 2019. However, rest  
489    of the time in absence of coherence in few months, patchiness takes over and the zooplankton  
490    biomass is erratic with sudden spikes and lasting bursts. This indicates that zooplankton form and  
491    patches fluctuate due to short-term changes, possibly responding to ocean environment [[Folt and](#)  
492    [Burns, 1999](#), [Raghukumar and Anil, 2003](#), [Anil et al., 2021](#)]. Hence, the zooplankton biomass much  
493    like the current is dominated by intraseasonal variations more than the annual cycle indicating  
494    possible loss in predictability.

495    Understanding the currents and phytoplankton variability and their relation to zooplankton  
496    would enable us to have better predictability. The occurrence of strong biomass intraseasonal  
497    variability before winter monsoon, along with similarity in the trend of increasing (decreasing)  
498    intraseasonal and intra-annual (annual) variability of biomass and currents as we go equatorward  
499    along the EAS slope is tempting, as it indicates a link between the two. However, a rigorous study  
500    is necessary to excavate any such relationship. Strong peaks in intraseasonal band in chl-a was  
501    evident in Lomb–Scargle periodogram (figure not shown), analogous to zooplankton biomass and

502 ZSS, but lacked concrete evidence of direct correlation.

### 503 5.3 Conclusion

504 The results presented in this paper are based on the ADCP backscatter which is suitable for creating  
505 long-term time series of zooplankton biomass in open ocean [Jiang et al., 2007, Hobbs et al., 2021,  
506 Ursella et al., 2021, Aparna et al., 2022]. There are however, certain limitations to this approach  
507 of studying biomass using ADCP backscatter as proxy. While the variation in depth is captured  
508 with in-situ samples from MPN, the variation in season is not adequately addressed owing to the  
509 limitation of months when ADCP servicing cruises are undertaken apart from availability. The west  
510 coast cruises for ADCP servicing are planned for the monsoon transition months but may start as  
511 early as late September till December with few exceptions such as 2022 when it was carried out  
512 in March. Since the intraseasonal and intra-annual variability is almost double that of the annual  
513 one ([section 4](#)), the sampling done in particular season for biomass-backscatter comparison isn't  
514 sufficient but can be mitigated with extensive season-wise sampling [[Jadhav and Smitha, 2024](#)].  
515 The second limitation is lack of any information regarding the size distribution of zooplankton and  
516 their contribution to ZSS is lost.

517 The merits outshine above mentioned disadvantages in the unique aspect that a sufficiently  
518 long and continuous time series of zooplankton biomass could be constructed upon which further  
519 analysis can be carried out. Along-with the discussion on seasonal and further the climatological  
520 cycle, we provided evidence of strong intraseasonal variation; this has three major implications:  
521 1) on the conventional sampling methods used to assess the zooplankton biomass and standing  
522 stock, and the snapshots provided by such samples aren't representative of a season; 2) on the  
523 zooplankton patchiness, and further on the under or over estimation of standing stock; 3) on the

524 predictability which is reduced due to strong biomass variation at intraseasonal scale, and the  
525 presence of patchiness as spikes and bursts. The possible influence of ocean currents could be  
526 explored using the current data from ADCPs [Hitchcock et al., 2002, Lawson et al., 2004]. It is  
527 evident that a mono-frequency ADCP is adequately suitable to capture the intraseasonal variations  
528 of zooplankton biomass that will otherwise be left inaccessible by traditional methods.

## 529 **6 Declaration of competing interest**

530 The authors declare that they have no known competing financial interests or personal relationships  
531 that could have appeared to influence the work reported in this paper.

## 532 **7 Acknowledgments**

533 The data were collected by xxx with fund provided under xxxx. The mooring programme is  
534 supported by INCOIS (Indian National Centre for Ocean Information Services, Hyderabad) and  
535 CSIR. We acknowledge the contribution of mooring division and ship cell of CSIR-NIO.

536 Ranjan Kumar Sahu expresses his acknowledgment to the Council of Scientific and Industrial  
537 Research (CSIR) for sponsoring his fellowship. Additionally, he extends his thanks to Ashok  
538 Kankonkar for providing the essential data, Rahul Khedekar for his data processing, Roshan D'Souza  
539 for his diligent work in biological data analysis. Their contributions were invaluable to the successful  
540 completion of this research.

## 541 **References**

542 Anna-Karin Almén and Tobias Tamelander. Temperature-related timing of the spring bloom and match between  
543 phytoplankton and zooplankton. *Marine Biology Research*, 16(8-9):674–682, 2020.

- 544 P Amol, D Shankar, SG Aparna, SSC Shenoi, V Fernando, SR Shetye, A Mukherjee, Y Agarvadekar, S Khalap, and  
545 NP Satelkar. Observational evidence from direct current measurements for propagation of remotely forced waves  
546 on the shelf off the west coast of india. *Journal of Geophysical Research: Oceans*, 117(C5), 2012.
- 547 P Amol, D Shankar, V Fernando, A Mukherjee, SG Aparna, R Fernandes, GS Michael, ST Khalap, NP Satelkar,  
548 Y Agarvadekar, et al. Observed intraseasonal and seasonal variability of the west india coastal current on the  
549 continental slope. *Journal of Earth System Science*, 123(5):1045–1074, 2014.
- 550 P Amol, Suchandan Bemal, D Shankar, V Jain, V Thushara, V Vijith, and PN Vinayachandran. Modulation of  
551 chlorophyll concentration by downwelling rossby waves during the winter monsoon in the southeastern arabian  
552 sea. *Progress in Oceanography*, 186:102365, 2020.
- 553 AC Anil, DV Desai, L Khandeparker, V Krishnamurthy, K Mapari, S Mitbavkar, JS Patil, VVSS Sarma, and  
554 SS Sawant. Short term response of plankton community to nutrient enrichment in central eastern arabian sea:  
555 Elucidation through mesocosm experiments. *Journal of Environmental Management*, 288:112390, 2021.
- 556 SG Aparna, DV Desai, D Shankar, AC Anil, Shrikant Dora, and R Khedekar. Seasonal cycle of zooplankton standing  
557 stock inferred from adcp backscatter measurements in the eastern arabian sea. *Progress in Oceanography*, 203:  
558 102766, 2022.
- 559 K Banse and DC English. Geographical differences in seasonality of czcs-derived phytoplankton pigment in the  
560 arabian sea for 1978–1986. *Deep Sea Research Part II: Topical Studies in Oceanography*, 47(7-8):1623–1677, 2000.
- 561 Karl Banse. Hydrography of the arabian sea shelf of india and pakistan and effects on demersal fishes. In *Deep sea*  
562 *research and oceanographic Abstracts*, volume 15, pages 45–79. Elsevier, 1968.
- 563 Karl Banse. Zooplankton: pivotal role in the control of ocean production: I. biomass and production. *ICES Journal*  
564 *of marine Science*, 52(3-4):265–277, 1995.
- 565 Richard T Barber, John Marra, Robert C Bidigare, Louis A Codispoti, David Halpern, Zackary Johnson, Mikel  
566 Latasa, Ralf Goericke, and Sharon L Smith. Primary productivity and its regulation in the arabian sea during  
567 1995. *Deep Sea Res. Part 2 Top. Stud. Oceanogr.*, 48(6-7):1127–1172, jan 2001.
- 568 H. P. Batchelder, J. R. VanKeuren, R. D. Vaillancourt, and E. Swift. Spatial and temporal distributions of acoustically  
569 estimated zooplankton biomass near the marine light-mixed layers station (59°30'n, 21°00'w) in the north atlantic  
570 in may 1991. *Journal of Geophysical Research: Oceans*, 100:6549–6563, 1995. doi: 10.1029/94jc00981.
- 571 Suchandan Bemal, Arga Chandrashekhar Anil, D Shankar, R Remya, and Rajdeep Roy. Picophytoplankton variability:  
572 Influence of winter convective mixing and advection in the northeastern arabian sea. *Journal of Marine Systems*,  
573 180:37–48, 2018.
- 574 John C Brock and Charles R McClain. Interannual variability in phytoplankton blooms observed in the northwestern  
575 arabian sea during the southwest monsoon. *Journal of Geophysical Research: Oceans*, 97(C1):733–750, 1992.

- 576 John C Brock, Charles R McClain, Mark E Luther, and William W Hay. The phytoplankton bloom in the north-  
577 western arabian sea during the southwest monsoon of 1979. *Journal of Geophysical Research: Oceans*, 96(C11):  
578 20623–20642, 1991.
- 579 Abhisek Chatterjee, D Shankar, SSC Shenoi, GV Reddy, GS Michael, M Ravichandran, VV Gopalkrishna,  
580 EP Rama Rao, TVS Udaya Bhaskar, and VN Sanjeevan. A new atlas of temperature and salinity for the north  
581 indian ocean. *Journal of Earth System Science*, 121:559–593, 2012.
- 582 Anya Chaudhuri, D Shankar, SG Aparna, P Amol, V Fernando, A Kankonkar, GS Michael, NP Satelkar, ST Khalap,  
583 AP Tari, et al. Observed variability of the west india coastal current on the continental slope from 2009–2018.  
584 *Journal of Earth System Science*, 129(1):57, 2020.
- 585 Anya Chaudhuri, P Amol, D Shankar, S Mukhopadhyay, SG Aparna, V Fernando, and A Kankonkar. Observed  
586 variability of the west india coastal current on the continental shelf from 2010–2017. *Journal of Earth System  
587 Science*, 130:1–21, 2021.
- 588 Boris Cisewski, Volker H Strass, Monika Rhein, and Sören Krägesky. Seasonal variation of diel vertical migration  
589 of zooplankton from adcp backscatter time series data in the lazarev sea, antarctica. *Deep Sea Research Part I:  
590 Oceanographic Research Papers*, 57(1):78–94, 2010.
- 591 Kenneth O Coyle and George L Hunt Jr. Seasonal differences in the distribution, density and scale of zooplankton  
592 patches in the upper mixed layer near the. *Plankton Biol. Ecol*, 47(1):31–42, 2000.
- 593 Kent L Deines. Backscatter estimation using broadband acoustic doppler current profilers. In *Proceedings of the  
594 IEEE Sixth Working Conference on Current Measurement (Cat. No. 99CH36331)*, pages 249–253. IEEE, 1999.
- 595 SN DeSousa, M Dileepkumar, S Sardessai, VVSS Sarma, and PV Shirodkar. Seasonal variability in oxygen and  
596 nutrients in the central and eastern arabian sea. Indian Academy of Sciences, 1996.
- 597 A Edvardsen, D Slagstad, KS Tande, and P Jaccard. Assessing zooplankton advection in the barents sea using  
598 underway measurements and modelling. *Fisheries Oceanography*, 12(2):61–74, 2003.
- 599 Boris Espinasse, Meng Zhou, Yiwu Zhu, Elliott L Hazen, Ari S Friedlaender, Douglas P Nowacek, Dezhong Chu,  
600 and Francois Carlotti. Austral fall- winter transition of mesozooplankton assemblages and krill aggregations in an  
601 embayment west of the antarctic peninsula. *Marine Ecology Progress Series*, 452:63–80, 2012.
- 602 Charles N Flagg and Sharon L Smith. On the use of the acoustic doppler current profiler to measure zooplankton  
603 abundance. *Deep Sea Research Part A. Oceanographic Research Papers*, 36(3):455–474, 1989.
- 604 Carol L Folt and Carolyn W Burns. Biological drivers of zooplankton patchiness. *Trends in Ecology & Evolution*,  
605 14(8):300–305, 1999.
- 606 H. E. García, R. A. Locarnini, T. P. Boyer, J. I. Antonov, A. V. Mishonov, O. K. Baranova, M. M. Zweng, J. R.  
607 Reagan, and D. R. Johnson. Dissolved oxygen, apparent oxygen utilization, and oxygen saturation. *NOAA Atlas  
608 NESDIS 75*, 3, 2014.

- 609 Charles H Greene, Peter H Wiebe, Chris Pelkie, Mark C Benfield, and Jacqueline M Popp. Three-dimensional  
610 acoustic visualization of zooplankton patchiness. *Deep Sea Research Part II: Topical Studies in Oceanography*, 45  
611 (7):1201–1217, 1998.
- 612 Charles F Greenlaw. Acoustical estimation of zooplankton populations 1. *Limnology and Oceanography*, 24(2):  
613 226–242, 1979.
- 614 Davide Guerra, Katrin Schroeder, Mireno Borghini, Elisa Camatti, Marco Pansera, Anna Schroeder, Stefania  
615 Sparnocchia, and Jacopo Chiggiato. Zooplankton diel vertical migration in the corsica channel (north-western  
616 mediterranean sea) detected by a moored acoustic doppler current profiler. *Ocean Science*, 15(3):631–649, 2019.
- 617 James M Hamilton, Kate Collins, and Simon J Prinsenberg. Links between ocean properties, ice cover, and plankton  
618 dynamics on interannual time scales in the canadian arctic archipelago. *Journal of Geophysical Research: Oceans*,  
619 118(10):5625–5639, 2013.
- 620 Graeme C Hays. A review of the adaptive significance and ecosystem consequences of zooplankton diel vertical  
621 migrations. In *Migrations and Dispersal of Marine Organisms: Proceedings of the 37 th European Marine Biology  
622 Symposium held in Reykjavík, Iceland, 5–9 August 2002*, pages 163–170. Springer, 2003.
- 623 Karen J Heywood, S Scrope-Howe, and ED Barton. Estimation of zooplankton abundance from shipborne adcp  
624 backscatter. *Deep Sea Research Part A. Oceanographic Research Papers*, 38(6):677–691, 1991.
- 625 Gary L Hitchcock, Peter Lane, Sharon Smith, Jiangang Luo, and Peter B Ortner. Zooplankton spatial distributions  
626 in coastal waters of the northern arabian sea, august, 1995. *Deep Sea Research Part II: Topical Studies in  
627 Oceanography*, 49(12):2403–2423, 2002.
- 628 Laura Hobbs, Neil S Banas, Jonathan H Cohen, Finlo R Cottier, Jørgen Berge, and Øystein Varpe. A marine  
629 zooplankton community vertically structured by light across diel to interannual timescales. *Biology Letters*, 17(2):  
630 20200810, 2021.
- 631 Raleigh R Hood, Lynnath E Beckley, and Jerry D Wiggert. Biogeochemical and ecological impacts of boundary  
632 currents in the indian ocean. *Progress in Oceanography*, 156:290–325, 2017.
- 633 Ryuichiro Inoue, Minoru Kitamura, and Tetsuichi Fujiki. Diel vertical migration of zooplankton at the s 1 biogeo-  
634 chemical mooring revealed from acoustic backscattering strength. *Journal of Geophysical Research: Oceans*, 121  
635 (2):1031–1050, 2016.
- 636 Shirin J Jadhav and BR Smitha. Abundance distribution pattern of zooplankton associated with the eastern arabian  
637 sea monsoon system as detected by underwater acoustics and net sampling. *Acoustics Australia*, pages 1–22, 2024.
- 638 Songnian Jiang, Tommy D Dickey, Deborah K Steinberg, and Laurence P Madin. Temporal variability of zooplankton  
639 biomass from adcp backscatter time series data at the bermuda testbed mooring site. *Deep Sea Research Part I:  
640 Oceanographic Research Papers*, 54(4):608–636, 2007.

- 641 R Jyothibabu, NV Madhu, H Habeebrehman, KV Jayalakshmy, KKC Nair, and CT Achuthankutty. Re-evaluation  
642 of ‘paradox of mesozooplankton’ in the eastern arabian sea based on ship and satellite observations. *Journal of*  
643 *Marine Systems*, 81(3):235–251, 2010.
- 644 Myounghee Kang, Sunyoung Oh, Wooseok Oh, Dong-Jin Kang, SungHyun Nam, and Kyounghoon Lee. Acoustic  
645 characterization of fish and macroplankton communities in the seychelles-chagos thermocline ridge of the southwest  
646 indian ocean. *Deep Sea Research Part II: Topical Studies in Oceanography*, 213:105356, 2024.
- 647 Madhavan Girijkumari Keerthi, Matthieu Lengaigne, Marina Levy, Jerome Vialard, Vallivattathillam Parvathi,  
648 Clément de Boyer Montégut, Christian Ethé, Olivier Aumont, Iyyappan Suresh, Valiya Parambil Akhil, et al.  
649 Physical control of interannual variations of the winter chlorophyll bloom in the northern arabian sea. *Biogeosciences*,  
650 14(15):3615–3632, 2017.
- 651 Punam A Khandagale, Vaibhav D Mhatre, and Sujitha Thomas. Seasonal and spatial variability of zooplankton  
652 diversity in north eastern arabian sea along the maharashtra coast. *Journal of the Marine Biological Association*  
653 *of India*, 64(1):25–32, 2022.
- 654 S Kidwai and S Amjad. Zooplankton: pre-southwest and northeast monsoons of 1993 to 1994, from the north arabian  
655 sea. *Mar. Biol.*, 136(3):561–571, apr 2000.
- 656 S. Prasanna Kumar and Jayu Narvekar. Seasonal variability of the mixed layer in the central arabian sea and its  
657 implication on nutrients and primary productivity. *Deep Sea Research Part II: Topical Studies in Oceanography*,  
658 52(14):1848–1861, 2005. ISSN 0967-0645. doi: <https://doi.org/10.1016/j.dsr2.2005.06.002>. URL <https://www.sciencedirect.com/science/article/pii/S0967064505001207>. Biogeochemical Processes in the Northern Indian  
659 Ocean.
- 660 Gareth L Lawson, Peter H Wiebe, Carin J Ashjian, Scott M Gallager, Cabell S Davis, and Joseph D Warren.  
661 Acoustically-inferred zooplankton distribution in relation to hydrography west of the antarctic peninsula. *Deep  
662 Sea Research Part II: Topical Studies in Oceanography*, 51(17-19):2041–2072, 2004.
- 663 Marina Lévy, D Shankar, J-M André, SSC Shenoi, Fabien Durand, and Clément de Boyer Montégut. Basin-wide  
664 seasonal evolution of the indian ocean’s phytoplankton blooms. *Journal of Geophysical Research: Oceans*, 112  
665 (C12), 2007.
- 666 M Li, A Gargett, and K Denman. What determines seasonal and interannual variability of phytoplankton and  
667 zooplankton in strongly estuarine systems? *Estuarine, Coastal and Shelf Science*, 50(4):467–488, 2000.
- 668 Yanliang Liu, Jingsong Guo, Yuhuan Xue, Chalermrat Sangmanee, Huiwu Wang, Chang Zhao, Somkiat Khokiat-  
669 tiwong, and Weidong Yu. Seasonal variation in diel vertical migration of zooplankton and micronekton in the  
670 andaman sea observed by a moored adcp. *Deep Sea Research Part I: Oceanographic Research Papers*, 179:103663,  
671 2022.
- 672 M Madhupratap, P Haridas, Neelam Ramaiah, and CT Achuthankutty. Zooplankton of the southwest coast of india:  
673 abundance, composition, temporal and spatial variability in 1987. 1992.

- 675 M Madhupratap, TC Gopalakrishnan, P Haridas, KKC Nair, PN Aravindakshan, G Padmavati, and Shiney Paul.  
676 Lack of seasonal and geographic variation in mesozooplankton biomass in the arabian sea and its structure in the  
677 mixed layer. *Current science. Bangalore*, 71(11):863–868, 1996a.
- 678 M Madhupratap, S Prasanna Kumar, PMA Bhattathiri, M Dileep Kumar, S Raghukumar, KKC Nair, and N Rama-  
679 iah. Mechanism of the biological response to winter cooling in the northeastern arabian sea. *Nature*, 384(6609):  
680 549–552, 1996b.
- 681 M Madhupratap, TC Gopalakrishnan, P Haridas, and KKC Nair. Mesozooplankton biomass, composition and  
682 distribution in the arabian sea during the fall intermonsoon: implications of oxygen gradients. *Deep Sea Research*  
683 *Part II: Topical Studies in Oceanography*, 48(6-7):1345–1368, 2001.
- 684 JP McCreary, Raghu Murtugudde, Jerome Vialard, PN Vinayachandran, Jerry D Wiggert, Raleigh R Hood,  
685 D Shankar, and S Shetye. Biophysical processes in the indian ocean. *Indian Ocean biogeochemical processes*  
686 and ecological variability
- 687 Julian P McCreary, Pijush K Kundu, and Robert L Molinari. A numerical investigation of dynamics, thermodynamics  
688 and mixed-layer processes in the indian ocean. *Progress in Oceanography*, 31(3):181–244, 1993.
- 689 Julian P McCreary, Kevin E Kohler, Raleigh R Hood, and Donald B Olson. A four-component ecosystem model of  
690 biological activity in the arabian sea. *Progress in Oceanography*, 37(3-4):193–240, 1996.
- 691 S Mukhopadhyay, D Shankar, S G Aparna, and A Mukherjee. Observations of the sub-inertial, near-surface east  
692 india coastal current. *Cont. Shelf Res.*, 148:159–177, September 2017.
- 693 KKC Nair, M Madhupratap, TC Gopalakrishnan, P Haridas, and Mangesh Gauns. The arabian sea: physical  
694 environment, zooplankton and myctophid abundance. 1999.
- 695 PV Nair. Primary productivity in the indian seas. *CMFRI Bulletin*, 22:1–63, 1970.
- 696 Jeffrey M Napp, Lewis S Incze, Peter B Ortner, Deborah LW Siefert, and Lisa Britt. The plankton of shelikof strait,  
697 alaska: standing stock, production, mesoscale variability and their relevance to larval fish survival. *Fisheries*  
698 *Oceanography*, 5:19–38, 1996.
- 699 Lingyun Nie, Jianchao Li, Hao Wu, Wencho Zhang, Yongjun Tian, Yang Liu, Peng Sun, Zhenjiang Ye, Shuyang  
700 Ma, and Qinfeng Gao. The influence of ocean processes on fine-scale changes in the yellow sea cold water mass  
701 boundary area structure based on acoustic observations. *Remote Sensing*, 15(17):4272, 2023.
- 702 MD Ohman and H-J Hirche. Density-dependent mortality in an oceanic copepod population. *Nature*, 412(6847):  
703 638–641, 2001.
- 704 SA Piontkovski, R Williams, and TA Melnik. Spatial heterogeneity, biomass and size structure of plankton of the  
705 indian ocean: some general trends. *Marine ecology progress series*, pages 219–227, 1995.

- 706 Emmanuel Potiris, Constantin Frangoulis, Alkiviadis Kalampokis, Manolis Ntoumas, Manos Pettas, George Peti-  
707 hakis, and Vassilis Zervakis. Acoustic doppler current profiler observations of migration patterns of zooplankton  
708 in the cretan sea. *Ocean Science*, 14(4):783–800, 2018.
- 709 TG Prasad and N Bahulayan. Mixed layer depth and thermocline climatology of the arabian sea and western  
710 equatorial indian ocean. 1996.
- 711 SZ Qasim. Biological productivity of the indian ocean. 1977.
- 712 Corinne Le Quéré, Robbie M Andrew, Josep G Canadell, Stephen Sitch, Jan Ivar Korsbakken, Glen P Peters,  
713 Andrew C Manning, Thomas A Boden, Pieter P Tans, Richard A Houghton, et al. Global carbon budget 2016.  
714 *Earth System Science Data*, 8(2):605–649, 2016.
- 715 Seshagiri Raghukumar and AC Anil. Marine biodiversity and ecosystem functioning: A perspective. *Current Science*,  
716 84(7):884–892, 2003.
- 717 CP Ramamirtham and AVS Murty. Hydrography of the west coast of india during the pre-monsoon period of the  
718 year 1962—part 2: in and offshore waters of the konkan and malabar coasts. *Journal of the Marine Biological  
719 Association of India*, 7(1):150–168, 1965.
- 720 S Ramamurthy. Studies on the plankton of the north kanara coast in relation to the pelagic fishery. *Journal of  
721 Marine Biological Association of India*, 7(1):127–149, 1965.
- 722 Mehbuba Rehim and Mudassar Imran. Dynamical analysis of a delay model of phytoplankton–zooplankton interac-  
723 tion. *Applied Mathematical Modelling*, 36(2):638–647, 2012.
- 724 T. P. Rippeth and J. H. Simpson. Diurnal signals in vertical motions on the hebridean shelf. *Limnology and  
725 Oceanography*, 43:1690–1696, 1998. doi: 10.4319/lo.1998.43.7.1690.
- 726 John H Ryther, John R Hall, Allan K Pease, Andrew Bakun, and Mark M Jones. Primary organic production in  
727 relation to the chemistry and hydrography of the western indian ocean 1. *Limnology and Oceanography*, 11(3):  
728 371–380, 1966.
- 729 Henrike Schmidt, Rena Czeschel, and Martin Visbeck. Seasonal variability of the arabian sea intermediate circulation  
730 and its impact on seasonal changes of the upper oxygen minimum zone. *Ocean Science*, 16(6):1459–1474, 2020.
- 731 D Shankar, SSC Shenoi, RK Nayak, PN Vinayachandran, G Nampoothiri, AM Almeida, GS Michael, MR Ramesh  
732 Kumar, D Sundar, and OP Sreejith. Hydrography of the eastern arabian sea during summer monsoon 2002.  
733 *Journal of earth system science*, 114:459–474, 2005.
- 734 D Shankar, R Remya, PN Vinayachandran, Abhisek Chatterjee, and Ambica Behera. Inhibition of mixed-layer  
735 deepening during winter in the northeastern arabian sea by the west india coastal current. *Climate Dynamics*,  
736 47:1049–1072, 2016.

- 737 D Shankar, R Remya, AC Anil, and V Vijith. Role of physical processes in determining the nature of fisheries in the  
738 eastern arabian sea. *Progress in Oceanography*, 172:124–158, 2019.
- 739 SSC Shenoi, D Shankar, GS Michael, J Kurian, KK Varma, MR Ramesh Kumar, AM Almeida, AS Unnikrishnan,  
740 W Fernandes, N Barreto, et al. Hydrography and water masses in the southeastern arabian sea during march–june  
741 2003. *Journal of earth system science*, 114:475–491, 2005.
- 742 SR Shetye, AD Gouveia, SSC Shenoi, D Sundar, GS Michael, AM Almeida, and K Santanam. Hydrography and  
743 circulation off the west coast of india during the southwest monsoon 1987. 1990.
- 744 S.R. Shetye, A.D. Gouveia, S.S.C. Shenoi, G.S. Michael, D. Sundar, A.M. Almeida, and K. Santanam. The coastal  
745 current off western india during the northeast monsoon. *Deep Sea Research Part A. Oceanographic Research  
746 Papers*, 38(12):1517–1529, 1991. ISSN 0198-0149. doi: [https://doi.org/10.1016/0198-0149\(91\)90087-V](https://doi.org/10.1016/0198-0149(91)90087-V). URL  
<https://www.sciencedirect.com/science/article/pii/019801499190087V>.
- 748 SR Shetye, AD Gouveia, and SSC Shenoi. Does winter cooling lead to the subsurface salinity minimum off saurashtra,  
749 india? *Oceanography of the Indian Ocean*, pages 617–625, 1992.
- 750 Wei Shi and Menghua Wang. Phytoplankton biomass dynamics in the arabian sea from viirs observations. *Journal  
751 of Marine Systems*, 227:103670, 2022.
- 752 Houssem Smeti, Marc Pagano, Christophe Menkes, Anne Lebourges-Dhaussy, Brian PV Hunt, Valerie Allain, Martine  
753 Rodier, Florian De Boissieu, Elodie Kestenare, and Cherif Sammari. Spatial and temporal variability of zooplank-  
754 ton off n ew c aledonia (s outhwestern p acific) from acoustics and net measurements. *Journal of Geophysical  
755 Research: Oceans*, 120(4):2676–2700, 2015.
- 756 Sharon Smith, Michael Roman, Irina Prusova, Karen Wishner, Marcia Gowing, LA Codispoti, Richard Barber, John  
757 Marra, and Charles Flagg. Seasonal response of zooplankton to monsoonal reversals in the arabian sea. *Deep Sea  
758 Research Part II: Topical Studies in Oceanography*, 45(10-11):2369–2403, 1998.
- 759 SL Smith and M Madhupratap. Mesozooplankton of the arabian sea: patterns influenced by seasons, upwelling, and  
760 oxygen concentrations. *Progress in Oceanography*, 65(2-4):214–239, 2005.
- 761 Patnaik Sreenivas, KVKRK Patnaik, and KVSR Prasad. Monthly variability of mixed layer over arabian sea using  
762 argo data. *Marine Geodesy*, 31(1):17–38, 2008.
- 763 R Subrahmanyam. Studies on the phytoplankton of the west coast of india: Part ii. physical and chemical factors  
764 influencing the production of phytoplankton, with remarks on the cycle of nutrients and on the relationship of  
765 the phosphate-content to fish landings. In *Proceedings/Indian Academy of Sciences*, volume 50, pages 189–252.  
766 Springer, 1959.
- 767 R Subrahmanyam and AH Sarma. Studies on the phytoplankton of the west coast of india. part iii. seasonal variation  
768 of the phytoplankters and environmental factors. *Indian Journal of Fisheries*, 7(2):307–336, 1960.

- 769 Laura Ursella, Vanessa Cardin, Mirna Batistić, Rade Garić, and Miroslav Gačić. Evidence of zooplankton vertical  
770 migration from continuous southern adriatic buoy current-meter records. *Progress in oceanography*, 167:78–96,  
771 2018.
- 772 Laura Ursella, Sara Pensieri, Enric Pallàs-Sanz, Sharon Z Herzka, Roberto Bozzano, Miguel Tenreiro, Vanessa Cardin,  
773 Julio Candela, and Julio Sheinbaum. Diel, lunar and seasonal vertical migration in the deep western gulf of mexico  
774 evidenced from a long-term data series of acoustic backscatter. *Progress in Oceanography*, 195:102562, 2021.
- 775 V Vijith, PN Vinayachandran, V Thushara, P Amol, D Shankar, and AC Anil. Consequences of inhibition of mixed-  
776 layer deepening by the west india coastal current for winter phytoplankton bloom in the northeastern arabian sea.  
777 *Journal of Geophysical Research: Oceans*, 121(9):6583–6603, 2016.
- 778 V Vijith, SR Shetye, AD Gouveia, SSC Shenoi, GS Michael, and D Sundar. Circulation in the region of the west  
779 india coastal current in march 1994 hydrographic and altimeter data. *Journal of Earth System Science*, 131(1):  
780 16, 2022.
- 781 Ian P Wade and Karen J Heywood. Acoustic backscatter observations of zooplankton abundance and behaviour  
782 and the influence of oceanic fronts in the northeast atlantic. *Deep Sea Research Part II: Topical Studies in  
783 Oceanography*, 48(4-5):899–924, 2001.
- 784 Peter H Wiebe, Charles H Greene, Timothy K Stanton, and Janusz Burczynski. Sound scattering by live zooplankton  
785 and micronekton: empirical studies with a dual-beam acoustical system. *The Journal of the Acoustical Society of  
786 America*, 88(5):2346–2360, 1990.
- 787 Jerry D Wiggert, RR Hood, Karl Banse, and JC Kindle. Monsoon-driven biogeochemical processes in the arabian  
788 sea. *Progress in Oceanography*, 65(2-4):176–213, 2005.
- 789 Monika Winder and Daniel E Schindler. Climatic effects on the phenology of lake processes. *Global change biology*,  
790 10(11):1844–1856, 2004.
- 791 Karen F Wishner, Marcia M Gowing, and Celia Gelfman. Mesozooplankton biomass in the upper 1000 m in the  
792 arabian sea: overall seasonal and geographic patterns, and relationship to oxygen gradients. *Deep Sea Research  
793 Part II: Topical Studies in Oceanography*, 45(10-11):2405–2432, 1998.

Table 1: ADCP deployment details at the locations. The temporal resolution is 1 hour, bin size(vertical resolution) 4 m. All ADCPs are operated at 153.3 kHz. The moorings are at a water column depth of 950–1200 m on the continental slope and are serviced on yearly basis according to ship availability. The 6th column consists of Reference echo intensity (Er) for each beam, while the 7th column contains the corresponding RSSI conversion factor [Deines, 1999].

Station (Position; °E, °N)	Date		Depth			
	Deployment	Recovery	Ocean	ADCP	Er	Kc
Okha (67.47, 22.26)	01/10/2018	01/12/2019	996	118	37 , 37 , 37 , 36	0.42 , 0.44 , 0.42 , 0.43
	01/12/2019	04/12/2020	1166	312	39 , 36 , 38 , 36	0.42 , 0.44 , 0.42 , 0.43
	04/12/2020	08/03/2022	1021	144	41 , 37 , 38 , 37	0.42 , 0.44 , 0.42 , 0.43
	08/03/2022	01/01/2023	1019	142	37 , 38 , 39 , 36	0.42 , 0.44 , 0.42 , 0.43
Mumbai (69.24, 20.01)	09/11/2017	29/09/2018	1025	150	36 , 34 , 39 , 42	0.40 , 0.40 , 0.40 , 0.40
	29/09/2018	29/11/2019	1122	125	35 , 36 , 39 , 42	0.40 , 0.40 , 0.40 , 0.40
	29/11/2019	02/12/2020	1143	164	37 , 34 , 39 , 43	0.40 , 0.40 , 0.40 , 0.40
	02/12/2020	06/03/2022	1125	142	36 , 34 , 39 , 42	0.40 , 0.40 , 0.40 , 0.40
	07/03/2022	02/01/2023	1103	158	37 , 34 , 40 , 43	0.40 , 0.40 , 0.40 , 0.40
Jaigarh (71.12, 17.53)	27/10/2017	27/09/2018	1039	198	32 , 35 , 33 , 32	0.45 , 0.45 , 0.45 , 0.45
	27/09/2018	30/10/2019	1032	164	32 , 35 , 33 , 31	0.45 , 0.45 , 0.45 , 0.45
	03/11/2019	30/11/2020	1142	264	32 , 36 , 33 , 32	0.45 , 0.45 , 0.45 , 0.45
	30/11/2020	05/03/2022	1099	119	33 , 36 , 34 , 32	0.45 , 0.45 , 0.45 , 0.45
Goa (72.74, 15.17)	03/10/2017	25/09/2018	1000	174	35 , 37 , 34 , 35	0.44 , 0.44 , 0.40 , 0.41
	25/09/2018	16/10/2019	969	145	38 , 36 , 36 , 34	0.44 , 0.44 , 0.40 , 0.41
	16/10/2019	29/11/2020	966	143	44 , 38 , 36 , 43	0.44 , 0.44 , 0.40 , 0.41
	29/11/2020	03/03/2022	985	157	35 , 40 , 35 , 38	0.44 , 0.44 , 0.40 , 0.41
	03/03/2022	05/01/2023	984	159	35 , 38 , 35 , 34	0.44 , 0.44 , 0.40 , 0.41
Udupi (74.04, 12.5)	05/10/2017	06/10/2018	1028	176	44 , 46 , 29 , 35	0.45 , 0.45 , 0.45 , 0.45
	06/10/2018	18/10/2019	1027	179	32 , 38 , 30 , 36	0.45 , 0.45 , 0.45 , 0.45
	18/10/2019	11/12/2020	1018	168	33 , 37 , 31 , 38	0.45 , 0.45 , 0.45 , 0.45
	11/03/2022	06/01/2023	1036	155	31 , 32 , 32 , 33	0.45 , 0.45 , 0.45 , 0.45
Kollam (75.44, 9.05)	07/10/2017	08/10/2018	1174	200	43 , 55 , 45 , 43	0.49 , 0.50 , 0.49 , 0.50
	08/10/2018	20/10/2019	1160	123	49 , 62 , 46 , 46	0.49 , 0.50 , 0.49 , 0.50
	20/10/2019	13/12/2020	1209	176	52 , 61 , 54 , 55	0.49 , 0.50 , 0.49 , 0.50
	13/12/2020	13/03/2022	1129	91	49 , 51 , 46 , 47	0.49 , 0.50 , 0.49 , 0.50
	13/03/2022	08/01/2023	1149	164	41 , 48 , 43 , 41	0.49 , 0.50 , 0.49 , 0.50
Kanyakumari (77.39, 6.96)	16/11/2016	08/10/2017	1096	252	37 , 36 , 37 , 37	0.42 , 0.44 , 0.42 , 0.43
	08/10/2017	10/10/2018	1055	181	32 , 34 , 38 , 35	0.45 , 0.45 , 0.45 , 0.45
	10/10/2018	22/10/2019	1075	180	36 , 34 , 39 , 36	0.45 , 0.45 , 0.45 , 0.45
	22/10/2019	14/12/2020	1060	167	33 , 35 , 36 , 35	0.45 , 0.45 , 0.45 , 0.45
	14/12/2020	14/03/2022	1184	287	34 , 36 , 36 , 35	0.45 , 0.45 , 0.45 , 0.45

Table 2:

Volumetric samples of zooplankton of various stations. The sampling depth range is standardised for later years for bin range of 0–25m, 25–50m, 50–75m, 75–100m, 100–150m. The abbreviations are in the following manner: Okha (O), Mumbai (M), Jaigarh (J), Goa (G), Udupi (U), Kollam (K), Kanyakumari (KK); The number tags corresponds to particular cruise of a station.

Sample number	Tag	Lat( $^{\circ}$ N)	Lon( $^{\circ}$ E)	Date	Time (IST)	Sampling depth range (m)
1-3	G1	15.18	72.79	25 Sep 18	452	50–25, 100–50, 150–100
4-6	G2	15.16	72.71	25 Sep 18	2108	50–25, 100–50, 150–100
7-10	G2	15.16	72.71	25 Sep 18	2137	40–20, 60–40, 80–60, 100–80
11-14	J1			26 Sep 18	2000	40–20, 60–40, 80–60, 100–80
15-17	J2			27 Sep 18	2000	50–25, 100–50, 150–100
18-21	J2			27 Sep 18	2100	40–20, 60–40, 80–60, 100–80
22-25	M1	20	69.19	28 Sep 18	2135	40–20, 60–40, 80–60, 100–80
26-27	M1	20	69.19	28 Sep 18	2205	50–25, 100–50
28-29	M2	20.01	69.2	29 Sep 18	2035	50–25, 100–50
30-33	M2	20.01	69.2	29 Sep 18	2057	40–20, 60–40, 80–60, 100–80
34-37	U1			5 Oct 18	2000	40–20, 60–40, 80–60, 100–80
38-40	U1			5 Oct 18	2100	50–25, 100–50, 150–100
41-43	U2			6 Oct 18	2000	50–25, 100–50, 150–100
44-47	U2			6 Oct 18	2100	40–20, 60–40, 80–60, 100–80
48-51	K1	9.06	75.42	8 Oct 18	421	40–20, 60–40, 80–60, 100–80
52-54	K1	9.06	75.42	8 Oct 18	449	50–25, 100–50, 150–100
55-56	K2	9.04	75.4	8 Oct 18	2027	50–25, 100–50
57-60	K2	9.04	75.4	8 Oct 18	2045	40–20, 60–40, 80–60, 100–80
61-64	G2	15.16	72.74	16 Oct 19	829	50–25, 75–50, 100–75, 150–100
65-67	G3	15.16	72.74	16 Oct 19	1812	50–25, 75–50, 100–75
68-70	K2	9.02	75.42	20 Oct 19	840	50–25, 75–50, 100–75
71-74	K3	9.04	75.43	20 Oct 19	1934	50–25, 75–50, 100–75, 150–100
75-78	KK1			22 Oct 19	742	50–25, 75–50, 100–75, 150–100
79-82	KK2			22 Oct 19	1925	50–25, 75–50, 100–75, 150–100
83-86	J1			30 Oct 19	324	50–25, 75–50, 100–75, 150–100
87-89	J2			4 Nov 19	946	75–50, 100–75, 150–100
90-92	M2	19.98	69.22	29 Nov 19	1434	50–25, 75–50, 100–75
93-96	M3	20.01	69.23	30 Nov 19	958	50–25, 75–50, 100–75, 150–100
97-100	O1	22.24	67.49	1 Dec 19	937	50–25, 75–50, 100–75, 150–100
101	O2	22.25	67.46	1 Dec 19	1957	150–100
102-105	G3	15.68	73.22	28 Nov 20	930	50–25, 75–50, 100–75, 150–100
105-108	G4	15.32	73.22	29 Nov 20	1558	50–25, 75–50, 100–75, 150–100
108-110	J2	17.85	71.21	30 Nov 20	1458	75–50, 100–75, 150–100
111-114	J3	17.91	71.21	1 Dec 20	1052	50–25, 75–50, 100–75, 150–100
115-118	M4	20.03	69.38	2 Dec 20	2016	50–25, 75–50, 100–75, 150–100
119-00	O2	22.41	67.8	4 Dec 20	953	150–100
120-123	O3	22.41	67.79	4 Dec 20	2011	50–25, 75–50, 100–75, 150–100
124-127	K3	9.11	75.72	12 Dec 20	2335	50–25, 75–50, 100–75, 150–100
128-131	K4	9.06	75.74	13 Dec 20	1507	50–25, 75–50, 100–75, 150–100
132-134	KK1	7.62	77.63	14 Dec 20	1226	50–25, 75–50
135-138	KK2	7.62	77.63	14 Dec 20	2047	50–25, 75–50, 100–75, 150–100
139-142	G4	15.32	73.21	3 Mar 22	823	50–25, 75–50, 100–75, 150–100
143-146	G5	15.68	73.21	4 Mar 22	1030	50–25, 75–50, 100–75, 150–100
147-150	M5	19.99	69.23	7 Mar 22	957	50–25, 75–50, 100–75, 150–100
151-154	O3	22.24	67.5	8 Mar 22	806	50–25, 75–50, 100–75, 150–100
155-158	U3	12.5	74.04	12 Mar 22	1156	50–25, 75–50, 100–75, 150–100
159-160	K4	9.04	75.42	13 Mar 22	1027	50–25, 75–50, 100–75
161-164	KK3	6.97	77.4	15 Mar 22	1220	50–25, 75–50, 100–75, 150–100

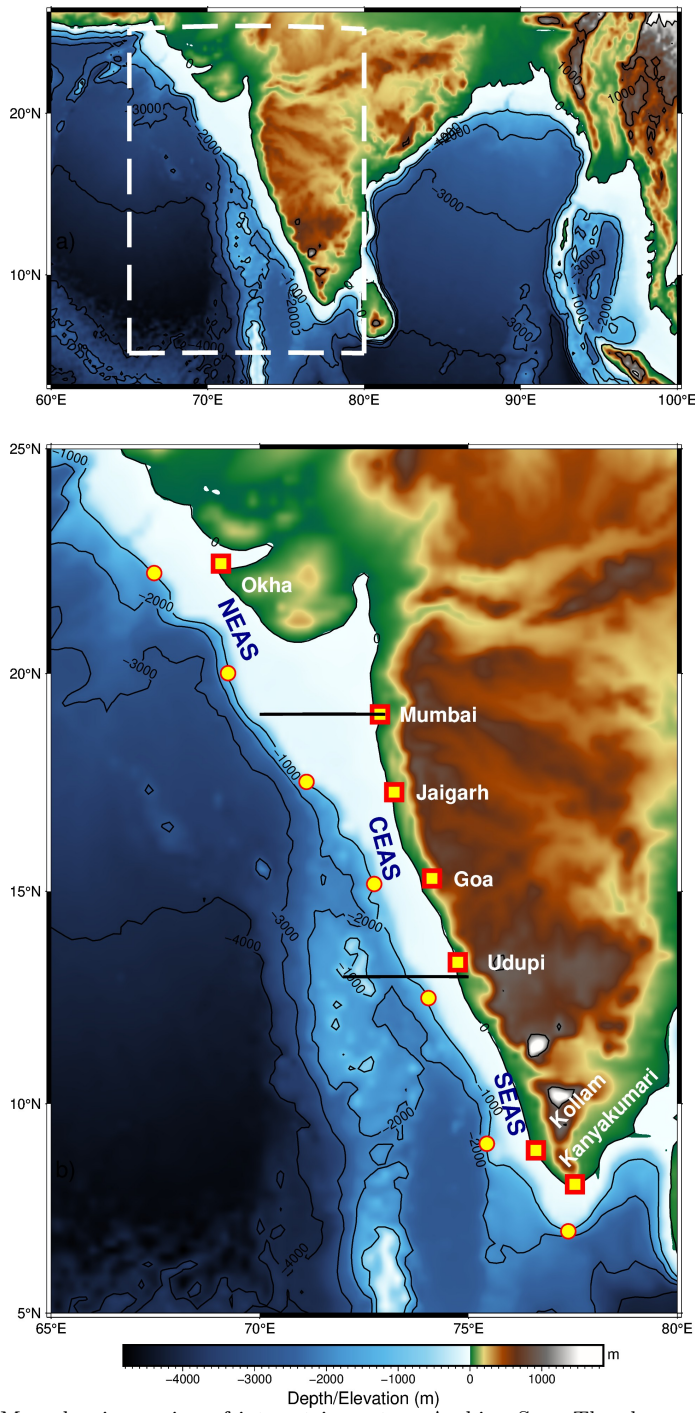


Figure 1: Map showing region of interest in eastern Arabian Sea. The slope moorings are deployed at  $\sim 1000$  m depth as shown in the bathymetry contour. Note the increase in shelf width as we go poleward along the coast. The mooring sites off Okha and Mumbai are in Northern EAS; Jaigarh and Goa in Central EAS while Kollam and Kanyakumari are at Southern EAS. Udupi is situated at the transition zone of Central and Southern EAS.

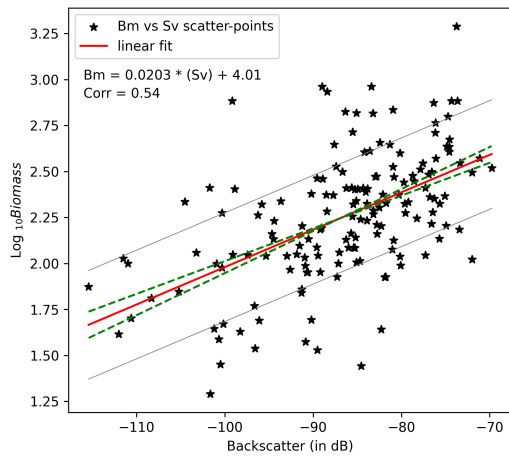


Figure 2: The linear fit line of Biomass ( $\log_{10}$  scale) and backscattering strength (in dB). The linear fit line is within the error range of previous result of [Aparna et al., 2022] (contained 67 data points) onto which latest zooplankton volumetric sample data (159 data points) is appended. The regression equation is  $y = (0.02 \pm 0.0025) x + (4.0144 \pm 0.2198)$  and correlation value of 0.54. The dashed green lines denote error range of plausible slope and intercept. From the linear equation, the upper and lower bound of error limit leads to an error bar of  $\sim 14 \text{ mg m}^{-3}$ . Standard deviation  $\sigma$  of  $\log_{10}(\text{Biomass})$  is  $\pm 0.49$ , which results in the backscatter range of 48.58 dB encompassing the entire backscatter range. It signifies the robustness of zooplankton biomass dependency on ADCP measured backscattering strength.

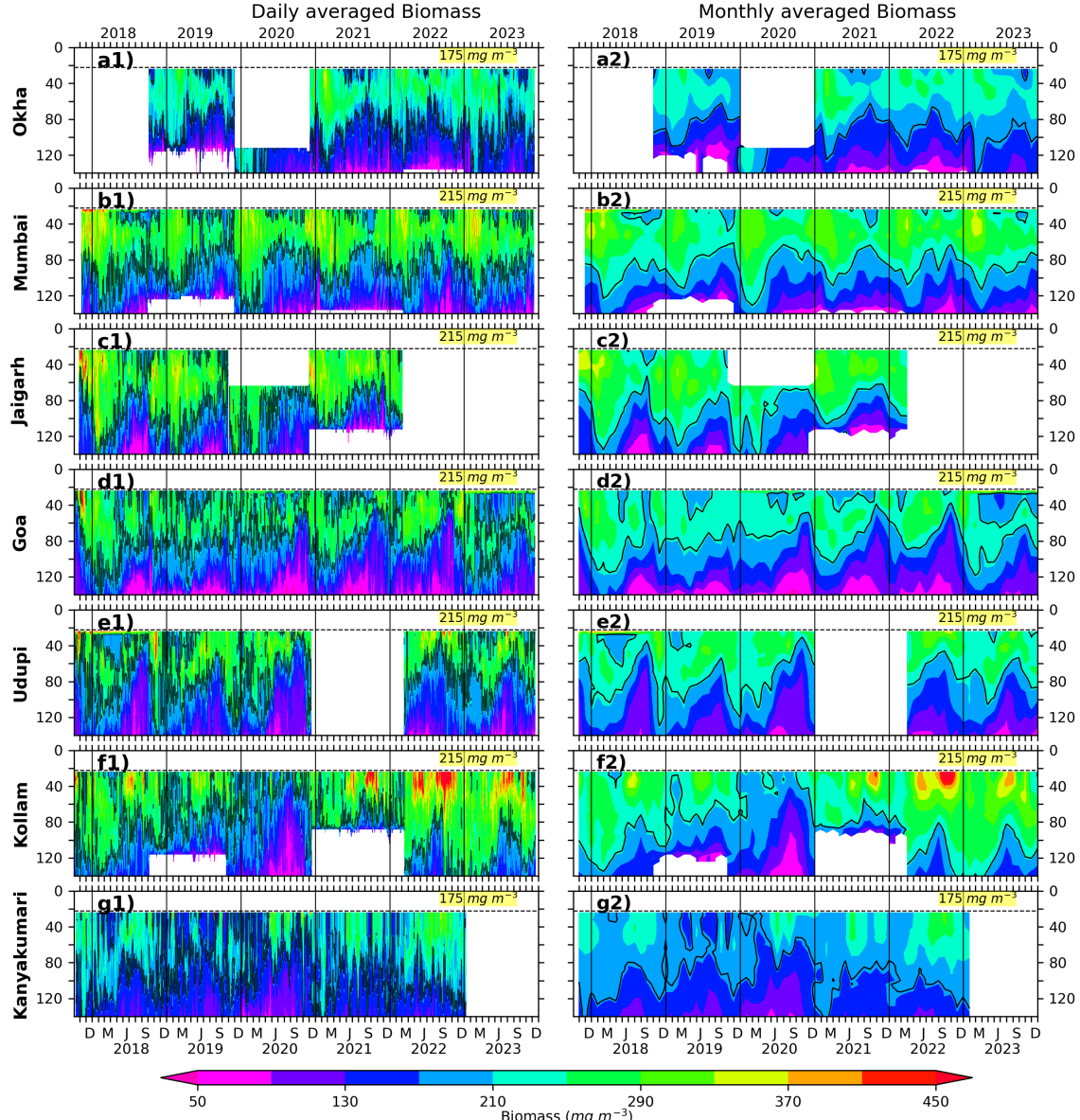


Figure 3: The Daily and monthly averaged biomass for EAS moorings, north (top) to south (bottom). The black contours are marking of  $175 \text{ mg m}^{-3}$  biomass for Okha and Kanyakumari;  $215 \text{ mg m}^{-3}$  for Mumbai, Goa and Kollam. The biomass contours are distinct and different based on the physico-chemical parameters and the one that best explains seasonality at respective location. The top 10% of data is discarded due to echo noise. The dashed line at 22 m marks the top-depth of first bin i.e, 24 m.

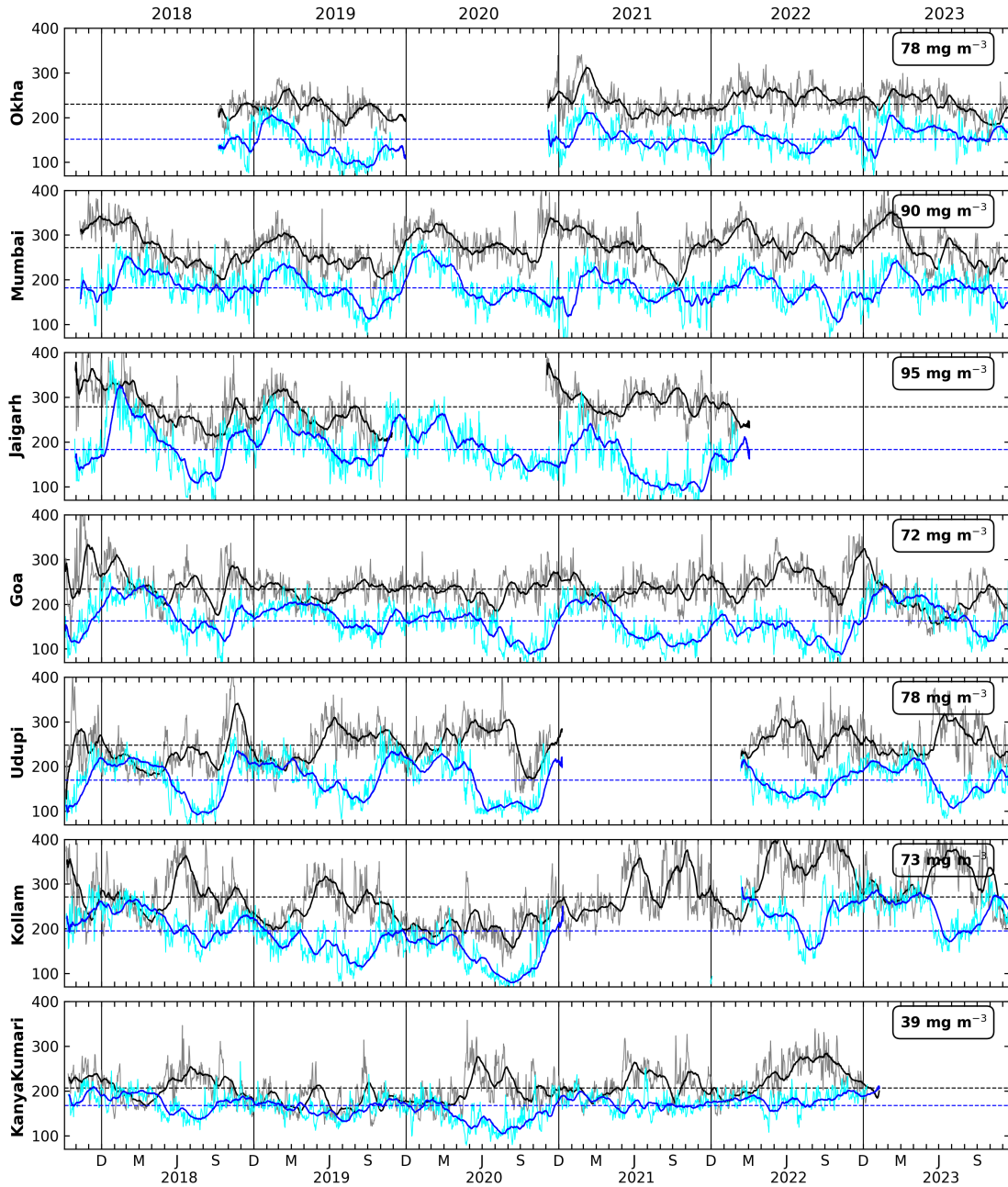


Figure 4: The daily biomass at depth of 40 m and 104 m for all locations shown by grey and cyan curves. The black and blue lines shows the 30 day rolling averaged biomass at 40 and 104 m, respectively. The difference in mean biomass at 40 and 104 is shown in top right box. Notice the spikes (bursts) seen in the daily (rolling mean) data of biomass at 40 m that lasts few days (few days to weeks), e.g., during many isolated days of June of 2020 (during entire June–July of 2020). These spikes and bursts are seen at all locations and both at 40 and 104 m, albeit with a varied magnitude.

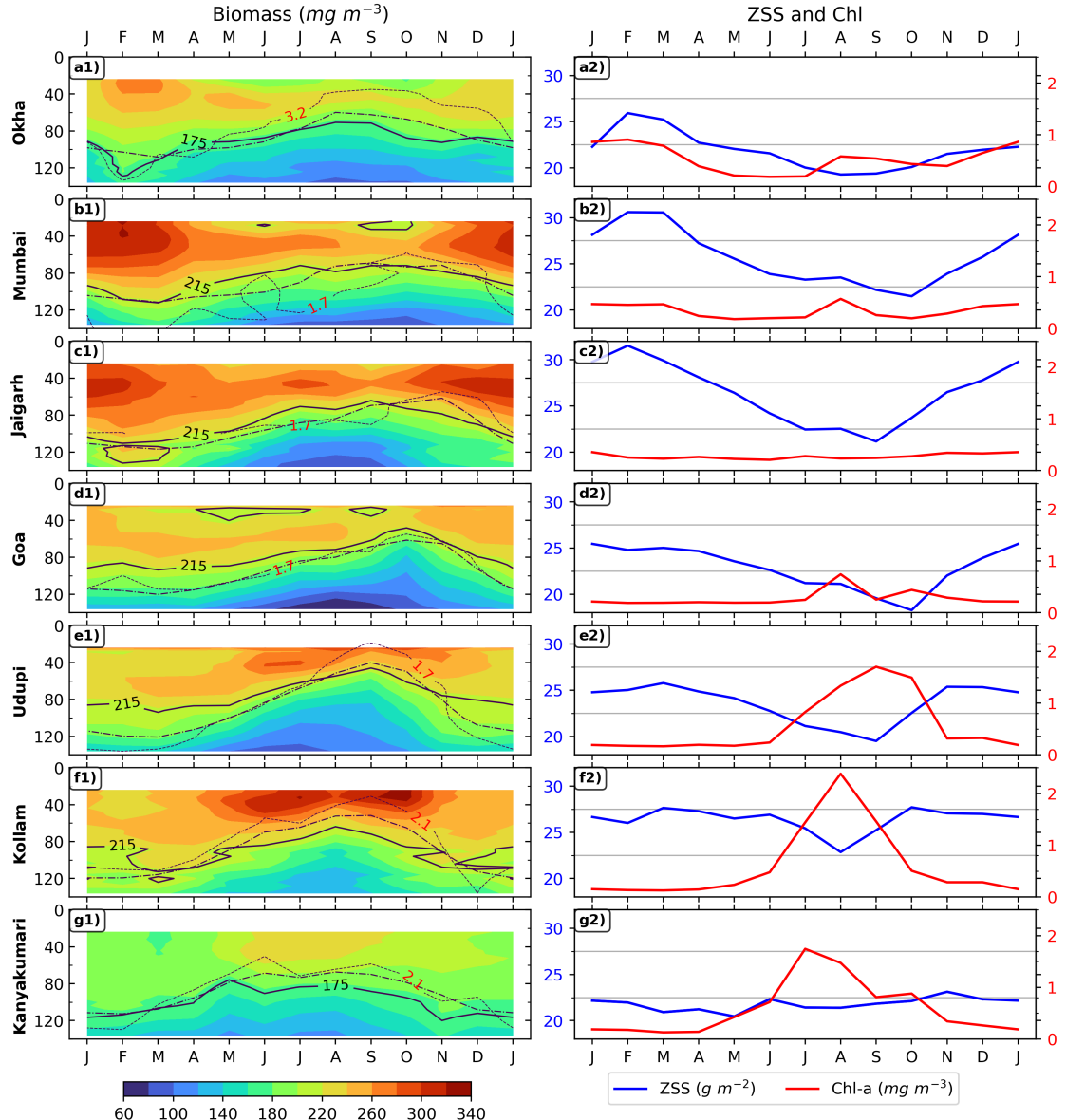


Figure 5: Monthly climatology of zooplankton biomass is shown in left panels for 7 locations, (top to bottom is southward). The D175 and D215 are shown in solid lines; dashed line represents the depth of 23 C isotherm; oxygen contours are shown in dotted lines and labeled for each mooring. The right set of panel plots is showing ZSS (24–140 biomass integral) and chl-a climatology for corresponding locations.

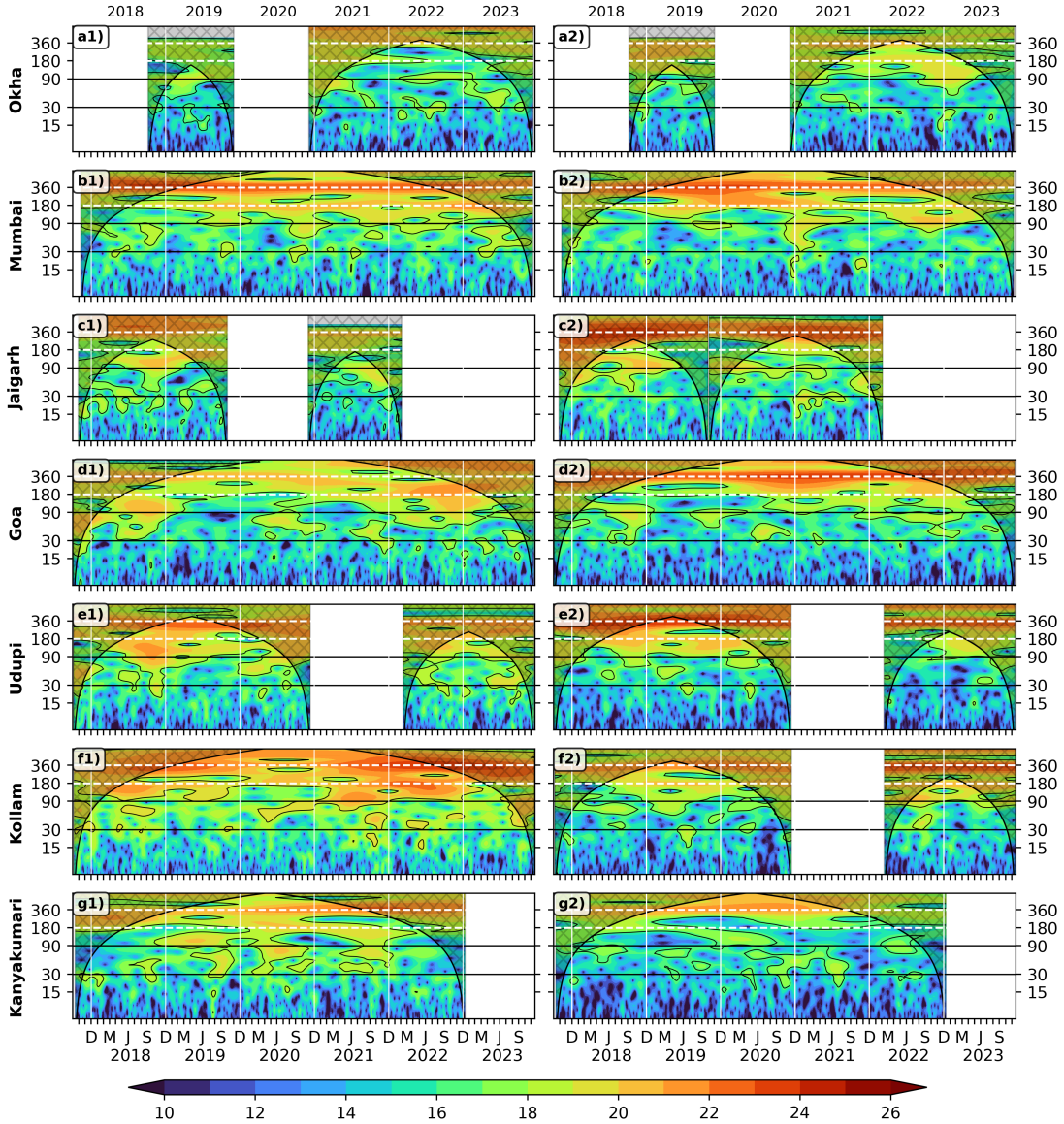


Figure 6: Wavelet power spectra (Morlet) of the 40 m (left panel) and 104 m (right panel) zooplankton biomass plotted against time as abscissa and period in days as ordinate. The wavelet power is in log<sub>2</sub> scale, the 95% significance is marked in black contours; the cross-shaded region falls under cone of influence. The horizontal dashed white (solid black) lines shows annual and semi-annual periods (intraseasonal band). Vertical white lines separates years.

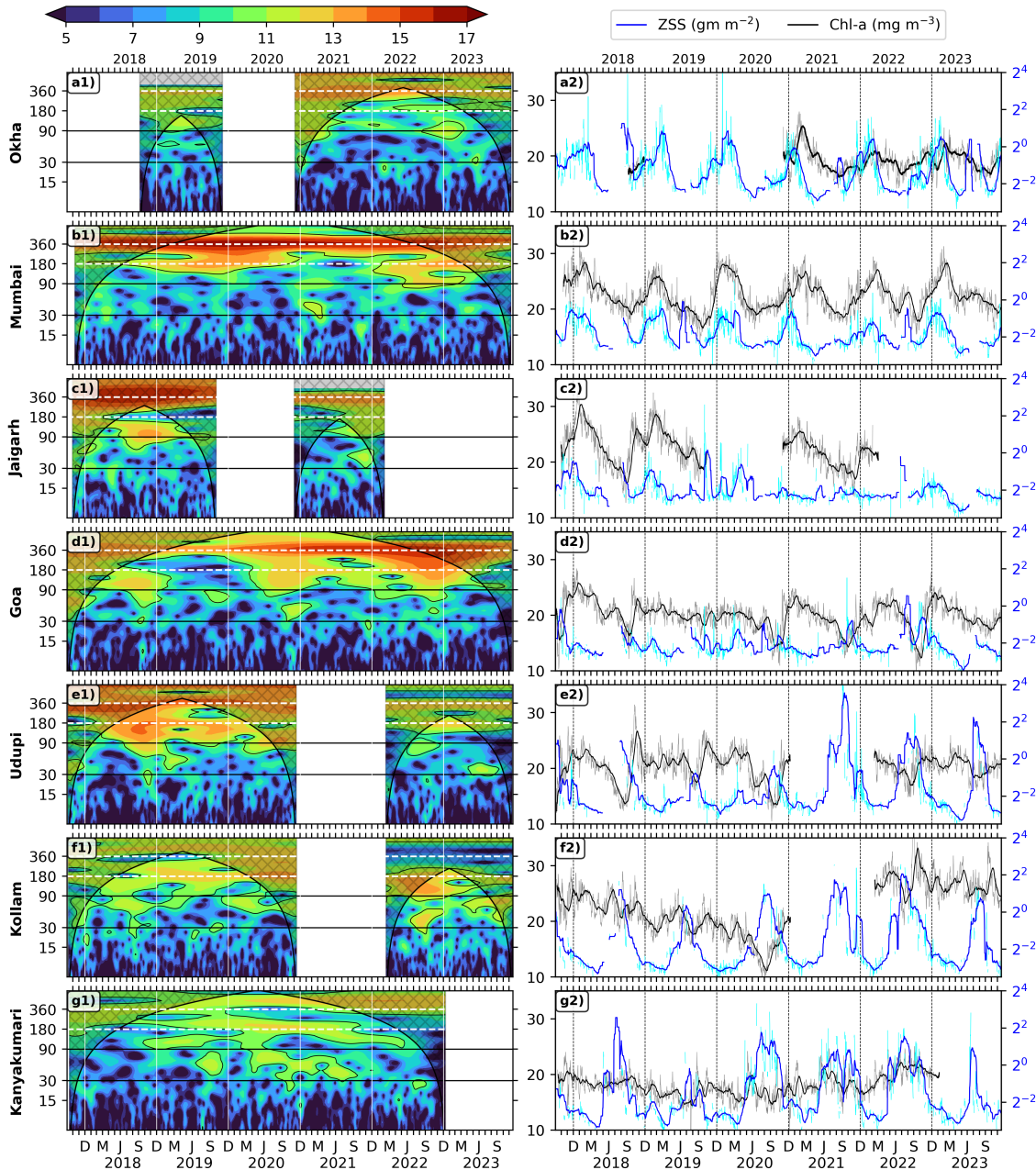


Figure 7: Wavelet power spectra (Morlet) of zooplankton standing stock plotted against time as abscissa and period in days as ordinate. The wavelet power is in  $\log_2$  scale, the 95% significance is marked in black contours; The vertical white lines separates years. The right side panel shows the ZSS (24–120 m biomass integral) time series of 30 day rolling mean data (black) overlaid upon daily data (Grey). The 30 day rolling mean data of chl-a (solid blue) is plotted over its daily data (cyan).

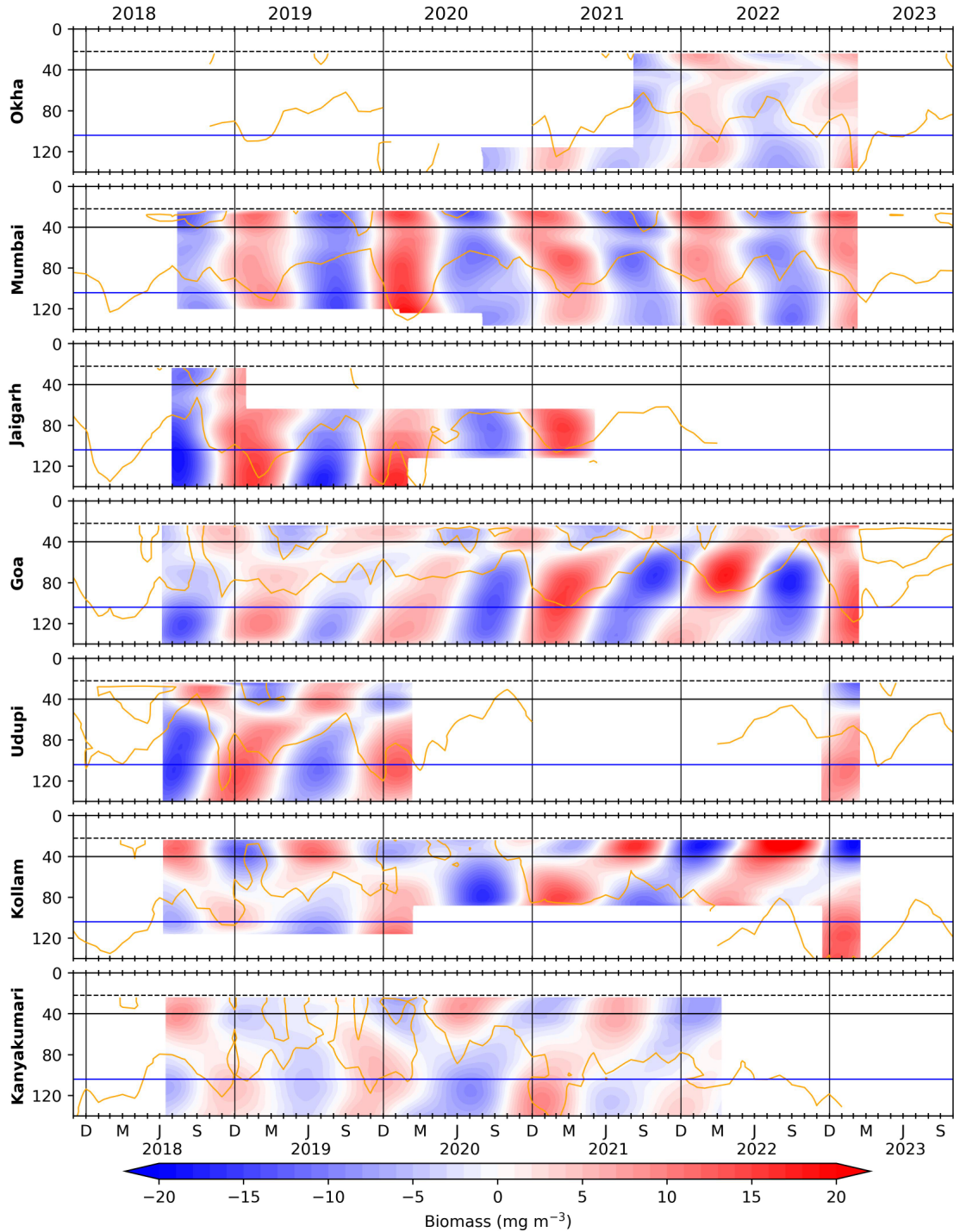


Figure 8: The biomass variation occurring in annual band (300 to 400 days). Owing to the presence of seasonal reversal of current, there is a variation driven by associated upwelling (downwelling) processes in summer (winter) monsoon. The horizontal black and blue lines are for 40 and 104 m, and the standard deviation of biomass at those depths are shown in respective colors at top right corner of each panel; vertical black lines separate the years. The dashed line at 22 m marks the top-depth of first bin i.e., 24 m and solid orange curves denote D215 (D175 off Okha and Kanyakumari)

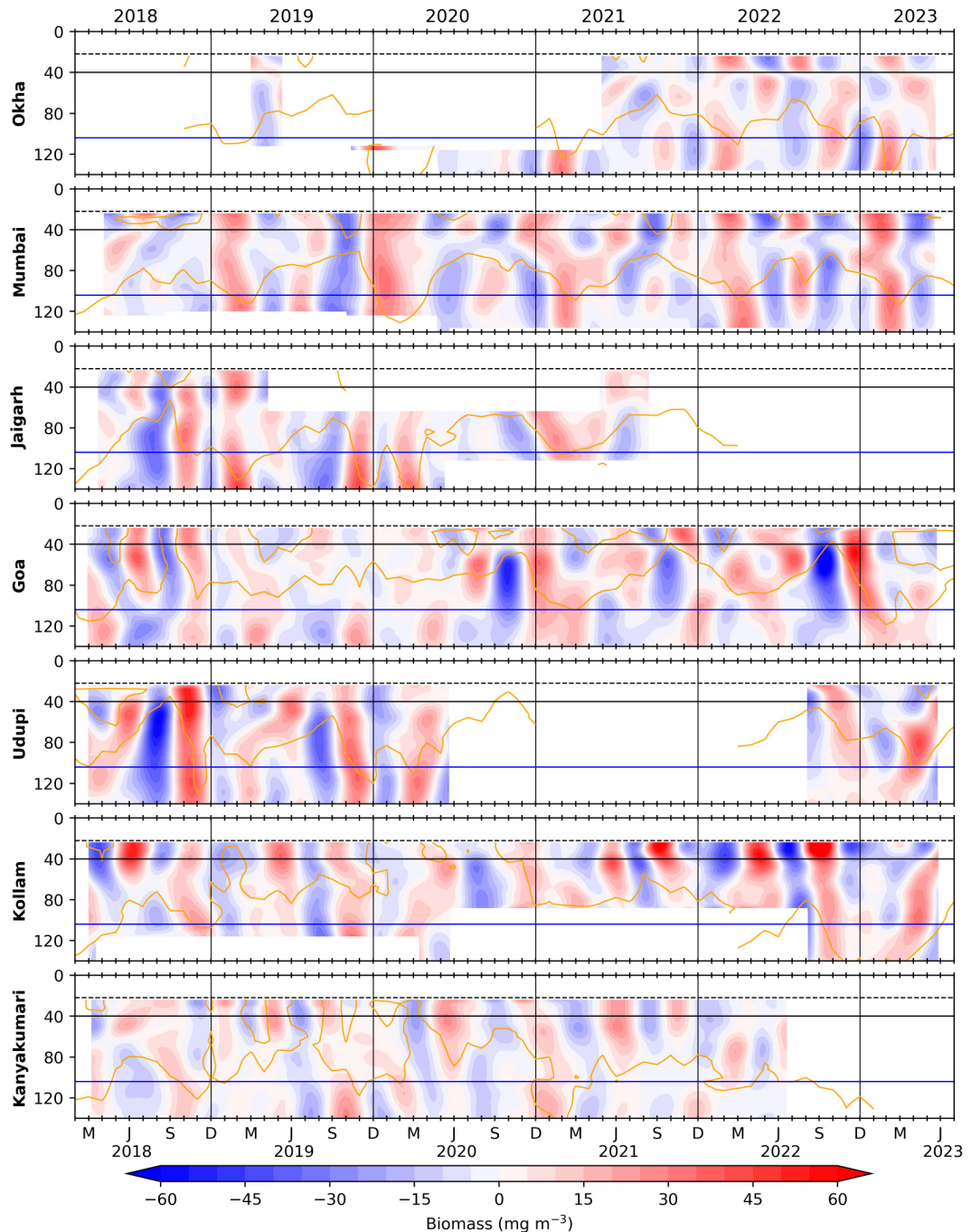


Figure 9: The biomass variation occurring in 100 to 250 days period (between the seasons and within a year record or intra-annual band) is obtained using a band pass filter. The horizontal black and blue lines is for 40 and 104 m, vertical black lines separate the years. The dashed line at 22 m marks the top-depth of first bin i.e, 24 m and solid orange curves denotes D215 (D175 off Okha and Kanyakumari).

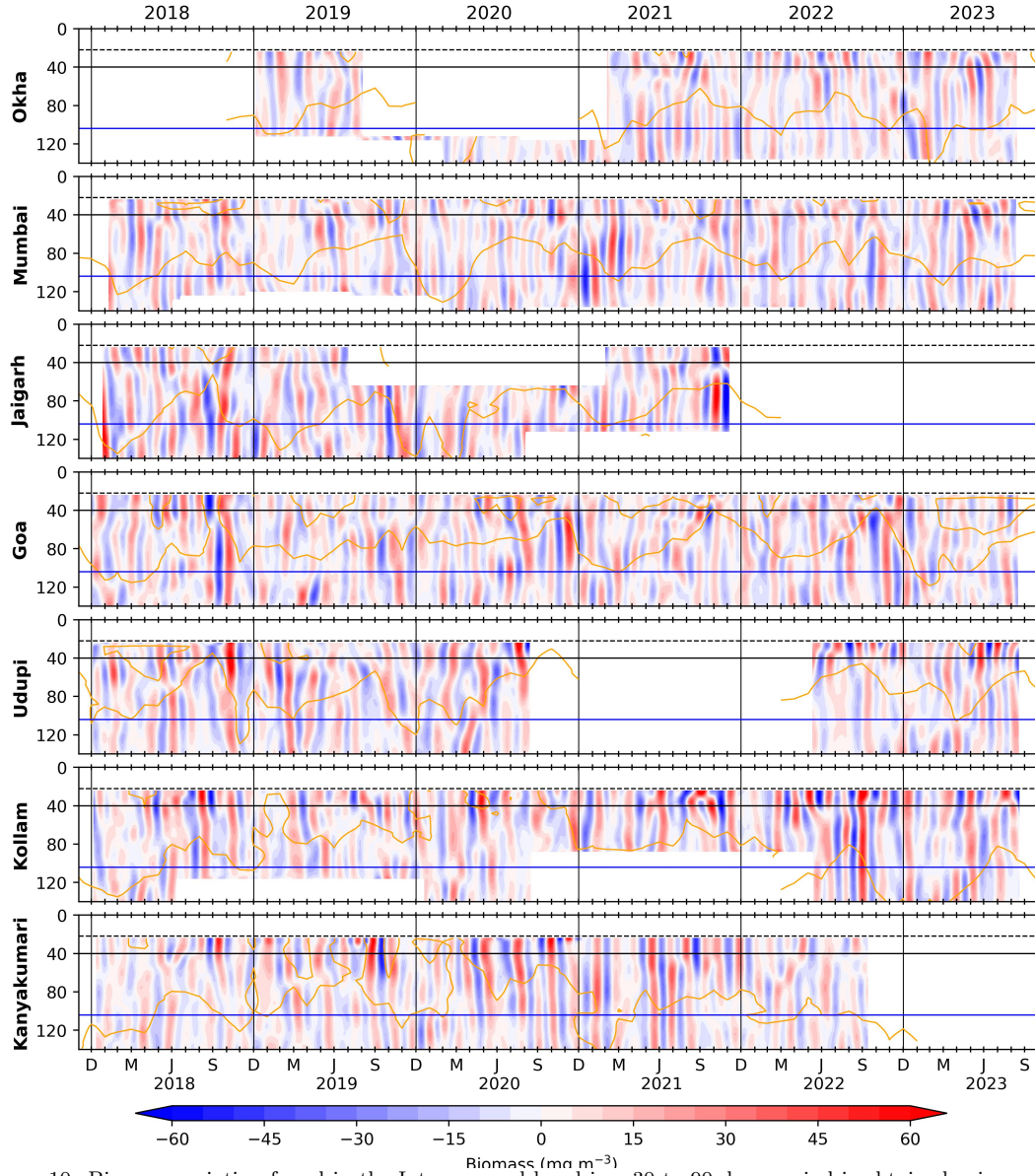


Figure 10: Biomass variation found in the Intraseasonal band i.e., 30 to 90 days period is obtained using a lanczos band pass filter. The horizontal black and blue lines is for 40 and 104 m; vertical black lines separate the years and solid orange curves denotes D215 (D175 off Okha and Kanyakumari). The dashed line at 22 m marks the top-depth of first bin i.e., 24 m. Intraseasonal variability is seen throughout the record, is coherent along the slope and its magnitude is stronger during August to November.

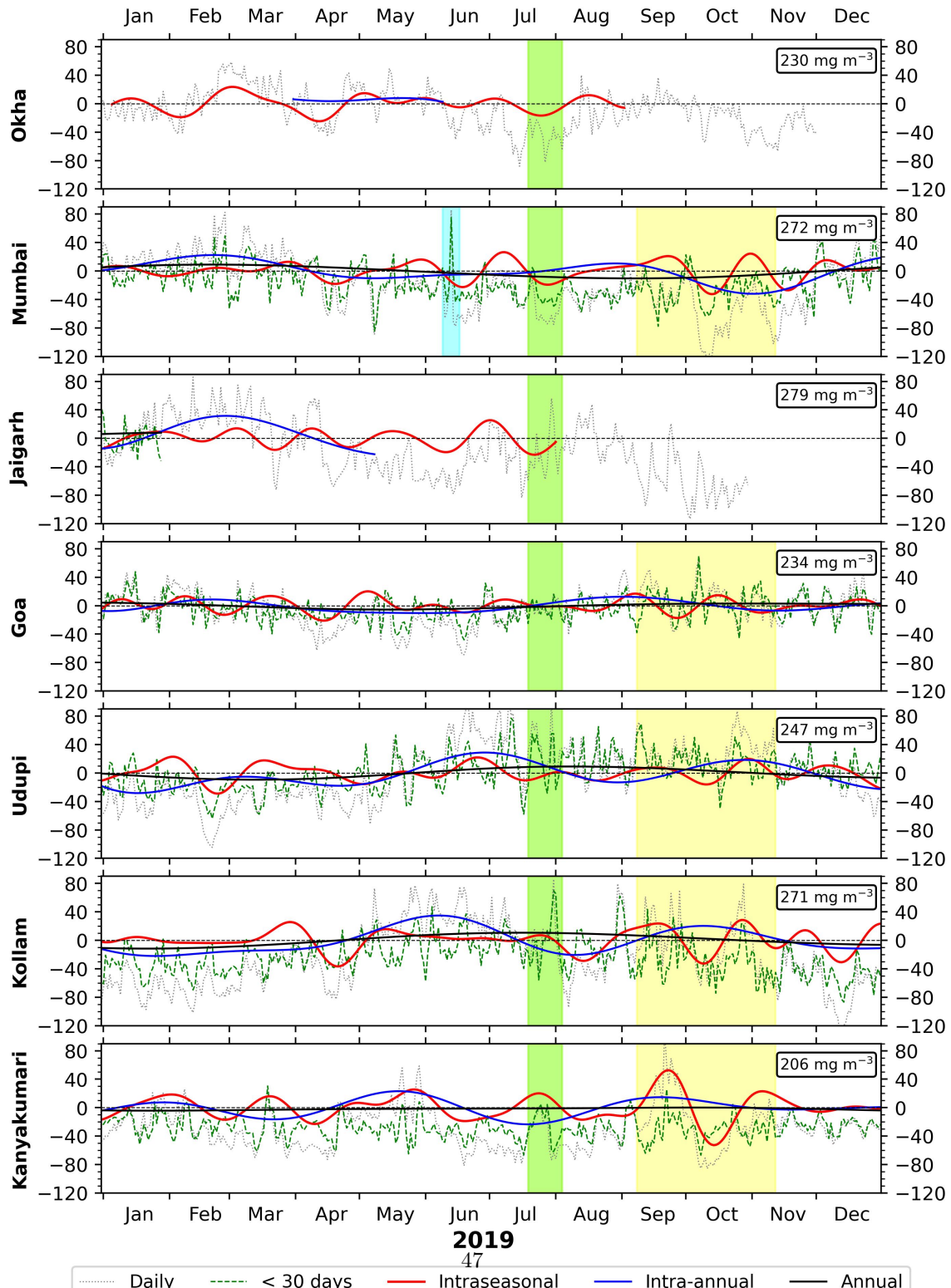


Figure 11: Comparison between mean-removed daily biomass time series at 40 m and the distinct components of variability off Mumbai, Goa and Kollam for 2019. The biomass units are  $\text{mg m}^{-3}$  and its mean for respective location is shown in top right box. Off Mumbai and Kollam, an increase in biomass is noticed from May onward and lasting till late monsoon with weeks of low biomass during August due to low contribution of intraseasonal component of variability. The yellow (green) highlighted region shows coherence in 30–90 days intraseasonal band (daily data) of 40 m biomass while the cyan shaded area shows a standalone spike (rapid increase in biomass in one to few days) that is not seen at adjacent mooring sites or nearby dates. The standalone spikes are representative of patchiness i.e., dense clusters of zooplankton and may not necessarily be observed elsewhere. The annual variability is very weak and lies close to zero almost always.